



Review

Aptamer-Based Optical and Electrochemical Sensors: A Review

Sidra Farid ^{1,*}, Shreya Ghosh ², Mitra Dutta ^{1,3} and Michael A. Stroscio ^{1,2}

¹ Department of Electrical and Computer Engineering, University of Illinois at Chicago, Chicago, IL 60607, USA; dutta@uic.edu (M.D.); stroscio@uic.edu (M.A.S.)

² Department of Bioengineering, University of Illinois at Chicago, Chicago, IL 60607, USA; shreyaghosh215@gmail.com

³ Department of Physics, University of Illinois at Chicago, Chicago, IL 60607, USA

* Correspondence: sfarid3@uic.edu

Abstract: There is a pressing need to identify recent directions in the field of aptamer-based sensing. DNA aptamers that are synthetically generated by in vitro selection mechanisms using the SELEX technique are single-stranded oligonucleotides which are selected to bind to a target with favorable sensitivity and selectivity. These aptamers have attracted significant attention due to their high binding affinity and ability to be easily engineered and provide various detection modes in what are known as aptasensors. Our aim is to focus on specialized detection strategies that have gained less attention but are of vital importance, such as optical detection in live cells, fluorescence polarization sensing, multi-analyte detection, colorimetric bioassays, wavelength shifting, and electrochemical-based detection. This will provide us with a perspective to facilitate developments in aptasensor technology for various targets, promising a bright future for biological receptors in the field of biosensing.

Keywords: electrochemical sensors; optical sensors; aptamers; FRET



Citation: Farid, S.; Ghosh, S.; Dutta, M.; Stroscio, M.A. Aptamer-Based Optical and Electrochemical Sensors: A Review. *Chemosensors* **2023**, *11*, 569. <https://doi.org/10.3390/chemosensors11120569>

Academic Editors: Pedro Salazar and Soledad Carinelli

Received: 13 October 2023

Revised: 11 November 2023

Accepted: 17 November 2023

Published: 21 November 2023



Copyright: © 2023 by the authors. Licensee MDPI, Basel, Switzerland. This article is an open access article distributed under the terms and conditions of the Creative Commons Attribution (CC BY) license (<https://creativecommons.org/licenses/by/4.0/>).

1. Introduction

The use of DNA and RNA has expanded not only in the advancements of genetic engineering and molecular biology, it has been rapidly evolving into a widespread field of technology including, but not limited to, the identification and detection of pathogenic agents, offering unprecedented synergies in the areas of biomedical research and clinical diagnostics [1,2]. Owing to the ultra-low concentrations of pathogenic agents in human fluids, such as blood, urine, etc., it is imperative to develop biosensors that possess selectivity and sensitivity for the effective treatment and earlier diagnosis of diseases. Biosensors in this domain are devices that contain a biological recognition element—called a *bioreceptor*—that is capable of recognizing target molecules [3]. These biological recognition elements transform signals that result from the interaction of a target with the biological element into information which is quantitative. These bioreceptors can exist in various forms such as aptamers, organic molecules such as peptides, antibodies, polymers, or various chemical molecules [4,5]; however, the aptamer as a recognition element in various sensing platforms is the focus of this article.

Aptamers, derived from the Latin word ‘*aptus*’, means ‘*to fit*’, were first recognized in 1990 by two groups, Ellington et al. [6] and Turek et al. [7], that reported earlier studies involving specific target affinity towards binding proteins. Nanoscale aptamers are short single-stranded DNA or RNA oligonucleotides that can bind to specific targets such as proteins, small molecules, cells, and even metal ions, for which antibodies are difficult to obtain with high affinity, thus serving as a versatile tool for target recognition and analyte detection in biological samples [8]. These aptamers can be utilized for the detection of specific analytes, as small- or large-scale molecules that are present at ultra-low concentrations due to their specific folding capabilities, in a variety of biological fluids or samples that

pertain interfering species by employing aptamer-based sensors or aptasensors. Along with this, the many unique characteristics of aptamers include, but are not limited to, longer shelf lives, simpler surface modifications, minor batch variations, and cost-effectiveness, which have led to significant efforts toward the development of aptasensors [9,10].

Figure 1 presents a chronological chart of key review article developments over the last decade on a range of important topics starting from the origin of aptamers [6,7] and aptasensors [10], along with pioneering review articles such as aptasensors in clinical diagnostics [11], for multi-analyte detection [12], biomedical applications of quantum dots [13], nanoparticles application in high-sensitive aptasensor design [14], aptasensors for organic pollutants and food and environment monitoring [15,16], aptasensors for prostate-antigen detection [17], disease-associated analyses of aptasensors [18], cytokine detection [19], and a recent article on Parkinson's disease-biomarkers-based aptasensors [20]. It is evident from this analysis that this review article is timely and needed to fill in the gap for a detailed analysis on recent advances and applications of specialized detection strategies that have gained less attention in the field of apta-biosensors, along with presenting a perspective and future directive for presenting the readers with a comprehensive review. We will summarize advances in the endocytosis of aptasensors for the detection of analytes in live cells, which is an important domain needed to be featured and highlighted, along with covering areas such as fluorescence polarization sensing, multi-analyte detection, colorimetric bioassays, wavelength shifting, and electrochemical-based detection. Specifically, our approach is as follows: first, we present the underlying mechanism of aptasensors, providing a retrospect of design strategies and immobilization methods on various substrates; we then give a synopsis on various assays' developments for the detection of analytes; and further present an outlook on comparisons of various detection strategies with an eye to the potential future endeavors, providing a sampling of directions for further research and developments.

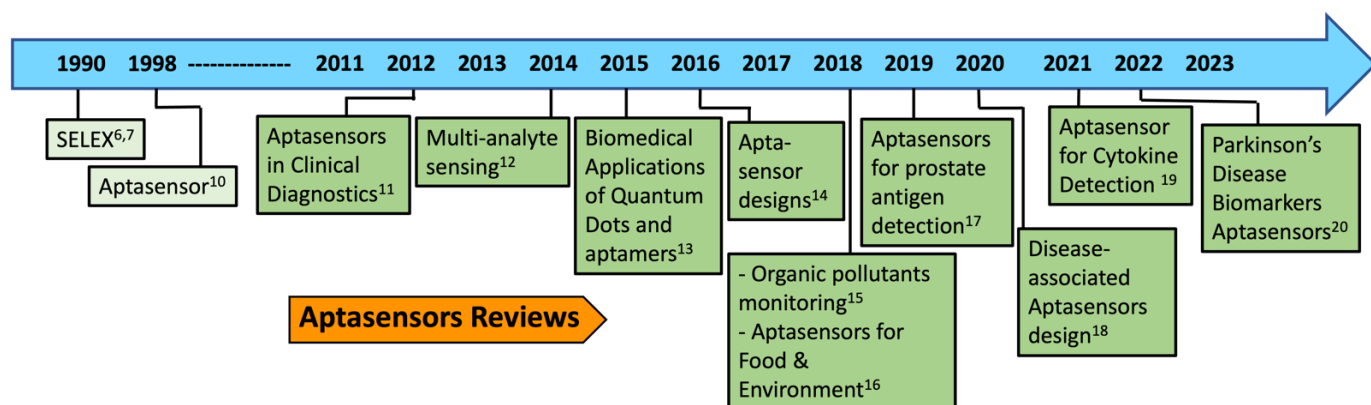


Figure 1. Pioneering review articles (below the timeline arrow) over the past decade in the field of aptasensors starting from origin of SELEX and aptasensors. The numbers in the boxes represent the references cited.

2. Aptamers: The Underlying Mechanism

Aptamers, specified as short single-stranded DNA or RNA oligonucleotides, show great binding affinity to a specific target molecule with high affinities. These aptamers are synthesized and incorporated through a well-known Systematic Evolution of Ligands by Exponential Enrichment (SELEX) process. In this experimental procedure, a progressive selection from a large nucleotide sequence possessing variable DNA binding affinities was made, which was subject to the target molecule. Using a repeated process of amplification, non-binding nucleotides were eliminated while only the binding nucleotides were amplified. The process was repeated over many rounds until an aptamer with desired properties was identified [21]. This is demonstrated in detail in the schematic described by Song et al. in Figure 2 [22]. Characterization techniques such as pull-down assays, gel electrophoresis,

capillary electrophoresis, particle display technology, bilayer interferometry, etc., are being used in addition to the SELEX procedure to further confirm selectivity [23,24].

Aptamers for biosensing own great advantages over antibodies, some of which include ease of functionalization, smaller size and versatility, reusability, a lack of additional processing steps, and unlimited shelf lives [24]. Some studies have compared aptamers with molecularly imprinted polymers for the recognition of proteins, which is an interesting read for biomimetic sensing [25]. However, in diagnostics, aptamers are well known and used to detect several different types of targets including metal ions like lead, calcium, and mercury, as well as biomolecules like interferon- γ , thrombin, glycated albumin, tumor necrosis factor- α (TNF- α), ATP, AMP, etc. [8–10]. Aptamers have also emerged as important tools for cancer diagnosis and have been studied to identify as few as 10 cancer cells. As targeting ligands, aptamers have been used to transport therapeutic reagents to targeted diseased organs/tumors. Slow off-rate-modified aptamers (SOMAMers) were developed by SomaLogic Inc. (Boulder, CO, USA) [26]. These modified aptamers were used for selecting aptamers against small molecules and challenging protein targets, such as toxins. They have been observed to display significantly higher affinity in the nanomolar to picomolar range, towards their targets.

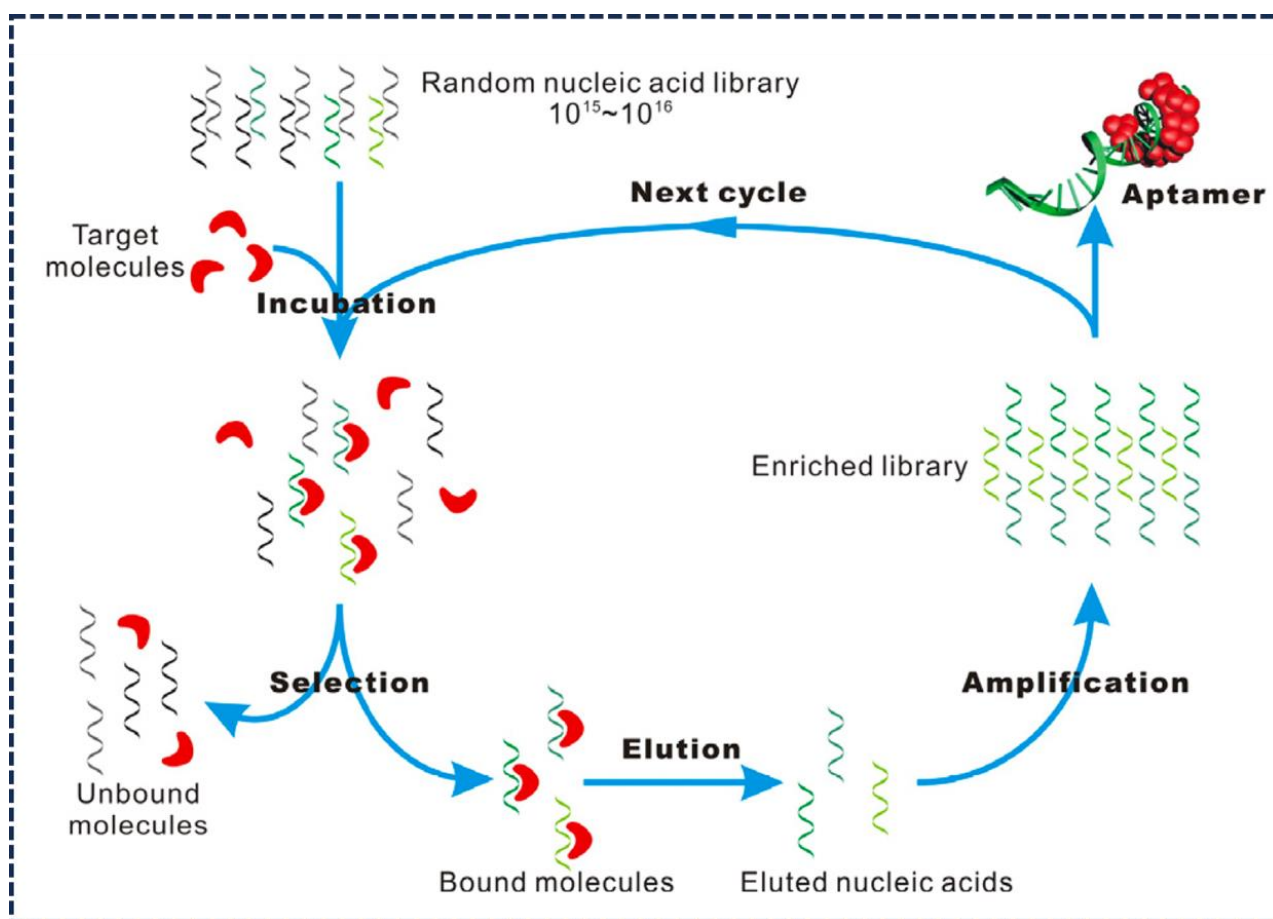


Figure 2. A schematic demonstrating the process of development of DNA aptamers using SELEX method [22].

3. Aptamer-Based Nanobiosensors Assay Formats

Aptamer-based bioassay formats have been a topic of particular attention due to their inherent advantages as mentioned earlier, alongside all the rapid progress of modern analytical technologies. Although there are three main kinds of aptasensors that are used traditionally, which include optical, electrochemical, and mass sensitive aptasensors, we

will cover in detail the optical detection techniques with a focus on specialized fluorescence-based detection strategies along with electrochemical-based detection. A conceptual model is shown in Figure 3, demonstrating the two detection methods for better visualization. Generally, optical detections that are based on fluorescence readouts are achieved by two elements, biorecognition molecule aptamers and signal transduction strategies. These aptasensors require a fluorophore and a quencher; the former is attached to one terminal of the aptamer while quencher is attached on the other end (Figure 3A) [15]. Upon aptamer binding to the target, a conformational change in the aptamer causes the fluorescence signal to change; this change can be correlated to the concentration of the target. Electrochemical detection, on the other hand, typically requires immobilization of the aptamer on an electrode. Binding of the aptamer to the target molecule causes an aptamer conformational change on the surface of electrode, resulting in a change in the current. This change in resistance can be correlated with the concentration of the target (Figure 3B) [15].

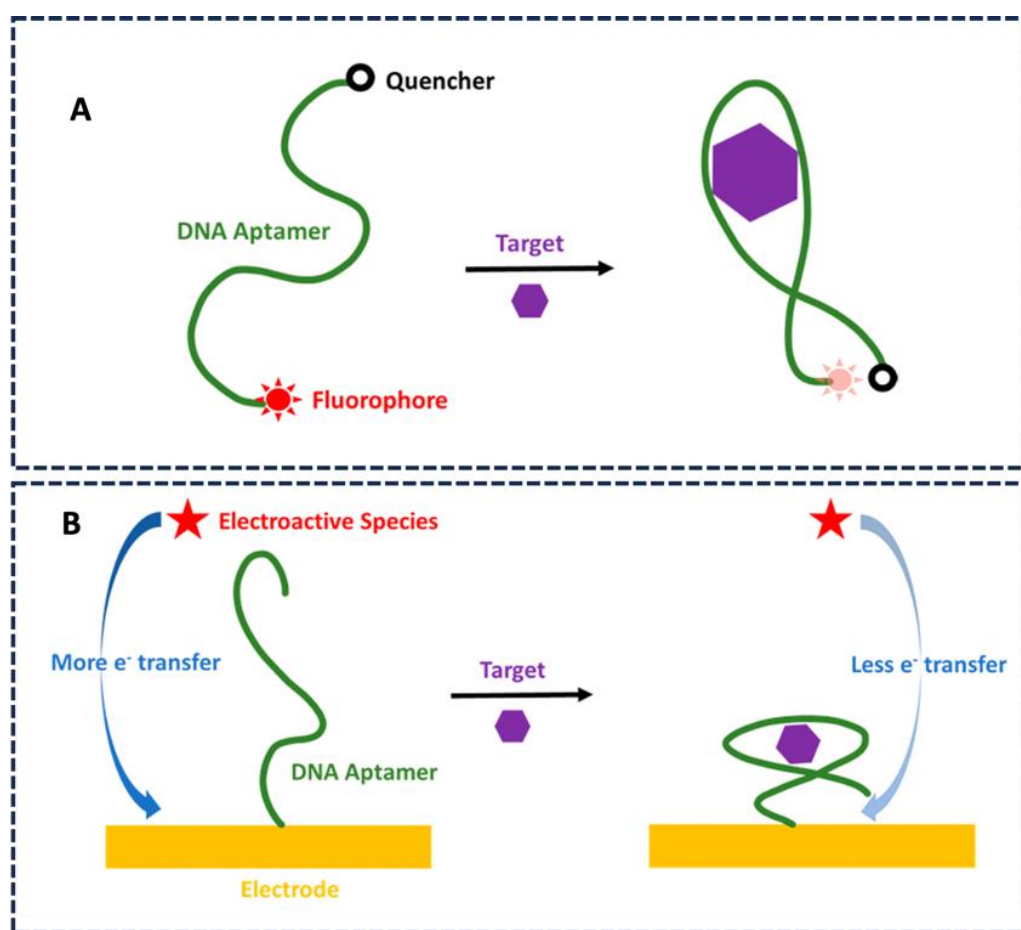


Figure 3. Conceptual models of a (A) fluorescence based sensor, and (B) electrochemical sensor [15]. (Reprinted (adapted) with permission from (Environmental science & technology 52, no. 16 (2018): 8989–9007) Copyright (2018) American Chemical Society.

3.1. Optical Detection

While there are many fluorescent response mechanisms, some of the strategies for signal transduction include Forster resonance energy transfer (FRET), fluorescence polarization (FP), fluorescence anisotropy (FA), aggregation-induced emission (AIE), etc. [27,28]. These fluorescent responses are triggered by specific interactions of the target molecule with the aptamers and the conformational changes they undergo.

3.1.1. FRET-Based Aptasensor in Live Cells

FRET is a non-radiative energy transfer process between an energy donor and an acceptor using intermolecular long-range dipole–dipole couplings [29]. A key attribute of FRET is the close proximity between an energy donor and acceptor, typically in the range of 1–10 nm, that holds an important role in the detection process. Strong FRET at small separations between the donor and acceptor has been discussed by Markvart et al. [30], who explains the radial dependence of the dipole–dipole interaction underlying FRET [30]. Such fluorescent aptasensors can be realized by choosing various fluorescent materials to fulfill this distance-dependence property of FRET-based aptasensors. FRET-based aptasensors have been used to detect various types of biomolecules such as proteins, enzymes, ions, etc. [31]. However, only a few studies have demonstrated their functioning in live cells [32]. This section focuses on such studies, where aptamer-based sensors utilize FRET to detect targets.

Ke Ma et al. in 2018 reported a fluorescent aptasensor based on aggregation-induced emission fluorogen (AIEgen) to detect ultra-small concentrations of intracellular interferon gamma (IFN- γ), as depicted in Figure 4A [33]. The proposed aptasensor was structured with an IFN- γ aptamer that was labeled with a fluorogen, which was capable of localizing interferon gamma in live cells during the secretion process in the cellular environment. The sensor exhibited a strong red emission on introduction of IFN- γ showing aggregation-induced emission, while the probe was nonfluorescent in the absence of IFN- γ . This aptasensor could detect ultra-low intracellular interferon gamma concentrations with the ability to localize intracellular IFN- γ as low as 10 pg mL^{-1} . Figure 4B shows the fluorescence curves of the TPE aptamer, which is a modified aptamer consisting of an AIEgen named TPEN3 and an oligonucleotide that shows high affinity to IFN- γ with various IFN- γ concentrations [33]. The aptasensor was able to detect intracellular IFN- γ with a lowest detection limit of 2 pg mL^{-1} and had the capacity of localizing IFN- γ in live cells during secretion. It was also observed to have excellent cellular permeability and biocompatibility as well as low cytotoxicity.

In a following study in 2021, Ke Ma et al. designed a graphene oxide (GO)-based fluorescent DNA nanomaterial for liver-cancer diagnosis and therapy (Figure 4C) [34]. This arrangement of nanomaterial consisted of a DNA tetrahedron, aptamers, the anti-tumor drug doxorubicin, and luminogens attached to the surface of GO. An aggregation-induced quench dye (Doxorubicin) and an aggregation-induced emission fluorescent probe (DSA) were introduced into the DNA structure. The sensor utilized the principle of FRET, which efficiently increased the emission intensity of DOX, resulting in bright red fluorescence of the constructed DNA nanomaterial. The DNA aptamers in the construct possess the ability to act as carriers for anti-tumor drugs such as Doxorubicin. Using GO as a quencher, this sensor utilizes the principle of FRET to specifically detect liver tumor cells and deliver the anticancer drug, hence proposing a promising cancer-theragnostic platform.

Jiayao et al. in a recent article in 2023 reported a DNAzyme nanoprobe for the catalytic imaging of proteins inside living cells [35]. This sensor consists of a DNAzyme subunit-containing aptamer hairpin along with another DNAzyme subunit adsorbed onto a molecular beacon substrate. When the intracellular protein target binds to the aptamer hairpin, the DNAzyme becomes activated and catalyzes the cleavage of the molecular beacon, which causes an increase in fluorescence. This sensor has been applied for monitoring the expression of nucleolin in living cells and is also able to differentiate between tumor cells and healthy living cells. Guo et al., on the other hand, developed a DNA nanopore, which was dually conjugated with a cell aptamer and cell-penetrating peptide [36]. The sequence of the aptamers was specifically bound to the Ramos cells, while the nanopore assembly entered into the cells with the help of a cell-penetrating membrane. This construct demonstrated the cellular uptake and selective targeting of Ramos cells.

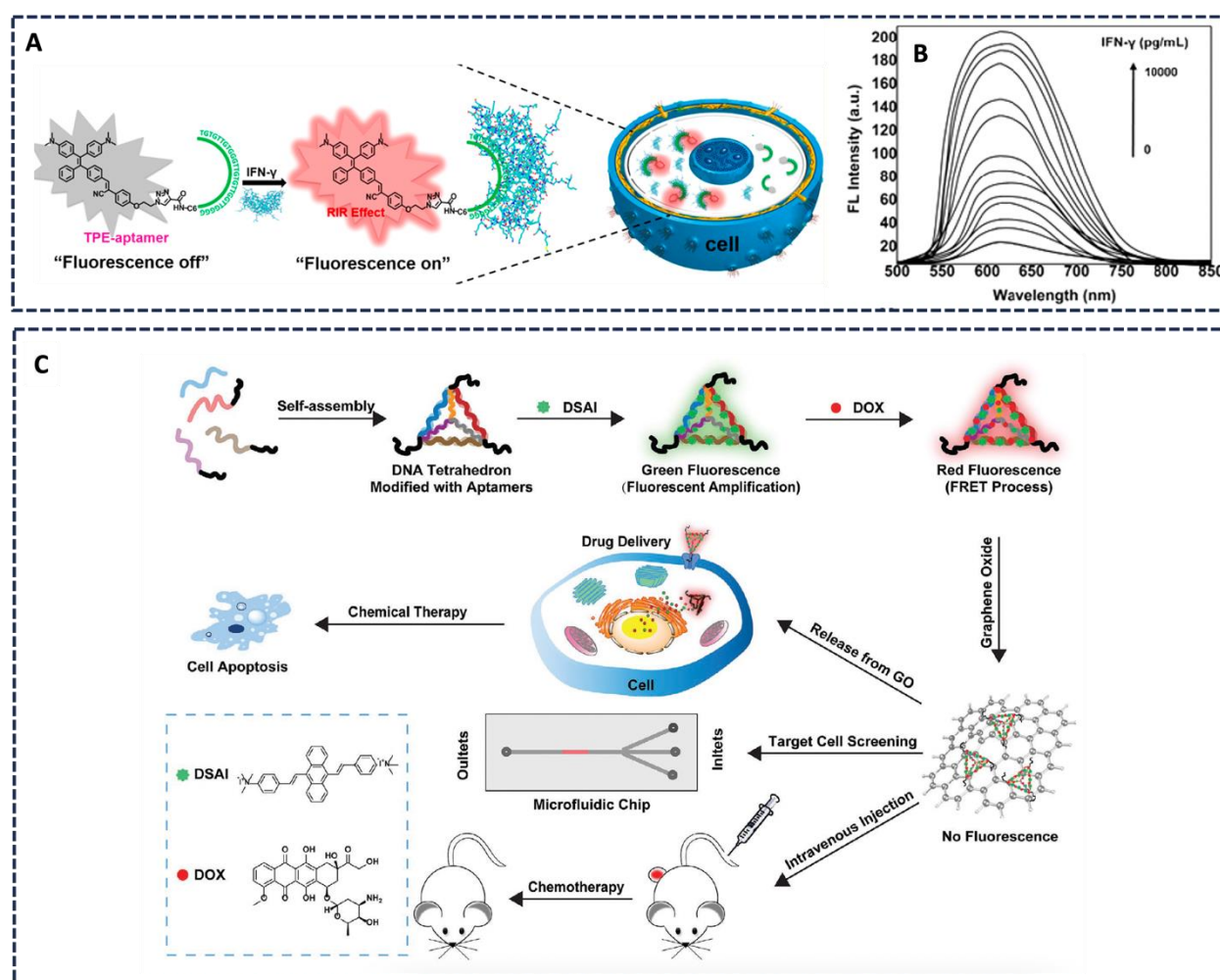


Figure 4. (A) AIEgen-based fluorescent aptasensor for the detection of intracellular IFN- γ . (Reprinted (adapted) with permission from [33] Copyright (2018) American Chemical Society.) (B) Fluorescence emission spectra with excitation at 415 nm and emission at 615 nm for TPE-aptamer at varied IFN- γ concentrations. (Reprinted (adapted) with permission from [33] Copyright (2018) American Chemical Society.) (C) Illustration of the GO-based fluorescent DNA construct for liver cancer theranostic. (Reprinted (adapted) with permission from [34] Copyright (2021) American Chemical Society).

Ghosh et al. [37] designed molecular beacons involving a quantum dot and gold nanoparticle, which were connected by a DNA aptamer. These molecular beacons were further conjugated with a cell-penetrating peptide (DSS), which is a set of amino acids like aspartic acid and serine, to allow for successful endocytosis of the apta-beacons. They reported studies on the detection of calcium ions as well as the detection of TNF- α in an intracellular environment. Using the principle of FRET, the sensitivity and specificity of these sensors were studied. In another study, Ghosh et al. [38] reported a study, where an optical DNA aptamer-based sensor was synthesized and characterized for the detection of calcium ions (Figure 5). The technique employed works on the principle of FRET and the aptasensor took a semiconductor quantum dot and Au nanoparticle as the donor–quencher pair. Upon calcium-ion binding, the DNA aptamer underwent a conformational change, causing an altered distance between the Au nanoparticle and the quantum dot. A limit of detection of 3.77 pM, along with a highly selective sensor, was fabricated for calcium ions as compared to other metal ions.

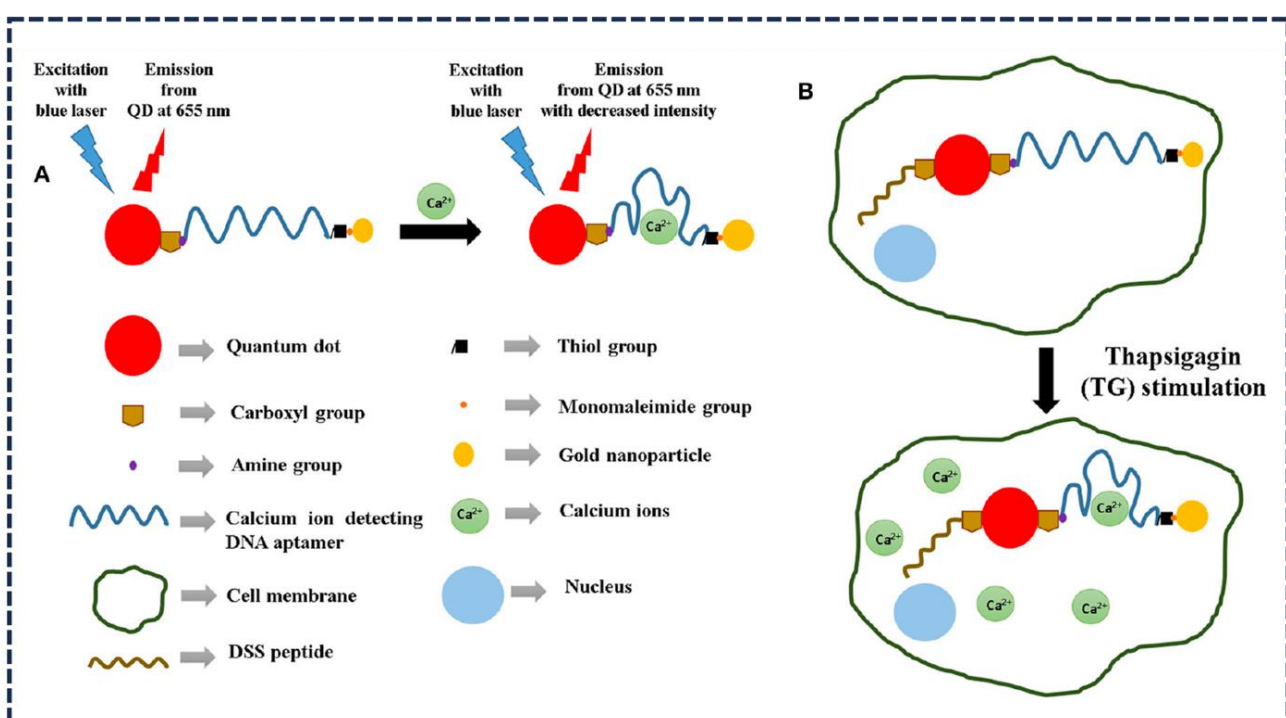


Figure 5. (A) Detection strategy for a FRET-based calcium biosensor, which is conjugated with a cell-penetrating peptide for cellular uptake [38]. (B) Illustration of an aptasensor-based detection strategy for the detection of calcium ions inside cells [38]. (© 2020 Ghosh, Chen, George, Dutta and Stroscio published under Creative Commons Attribution License (CC BY)).

3.1.2. Fluorescence Polarization Aptasensors

A new horizon that holds considerable promise for bioanalytical systems is fluorescence polarization-based bioassays. These are based on changes in fluorophore rotation after the interaction between an aptamer and target. The binding of an aptamer to a specific target may lead to a change in fluorescent polarization value, and the response can be regarded as a yardstick for quantitative target levels [39]. The underlying mechanism involves irradiating a reaction mixture with plane-polarized light and measuring the fluorescence induced by this irradiation. Polarized light will preferably be absorbed in a mixture of disordered molecules by those whose absorption oscillators are parallel with the polarization plane. In the case of an excited molecule not changing its orientation before emission, the fluorescence emission will also become polarized. This is explained in Figure 6 by Olga et al. [40]. In a comprehensive review they summarize and comparatively characterize the developments in the field of fluorescence polarization bioassays and the new techniques developed for detecting metal ions, enzymatic reactions, and nucleic acids.

These fluorescence polarization-based techniques using aptamers boast interest due to the production of aptamers of a given specificity in variably large quantities, giving researchers control over the selection of final aptamers by simply changing interaction conditions at various stages. Liu et al. [41] developed a simple and rapid fluorescence polarization-based bioassay to detect bisphenol A (BPA), which is one of the environmental endocrine disruptors that causes high risk to human health, devoted to the analysis of cocaine. By employing a single tetramethylrhodamine (TMR)-labeled short DNA aptamer against BPA, a change in fluorescence polarization was detected upon a conformational change in the labeled aptamer due to its binding with BPA. This caused a change in the interaction between guanine bases and TMR, achieving a detection limit of $0.5 \mu\text{mol L}^{-1}$ and good selectivity, as shown in Figure 7A,B. Pengfei Ma et al. [42] in a recent article developed a fluorescence polarization-based aptasensor for *Weissella viridescens* bacteria detection. Such predominant spoilage bacteria are commonly found in meat products

treated at low temperatures and ultrahigh pressures. Using SELEX methods, an aptamer TL43 with fewer bases and better affinity was generated to detect *W. viridescens*. A simple and rapid aptasensor that consisted of streptavidin, biotin-labeled TL43, and FAM-labeled cDNA was employed, which enhanced fluorescence polarization changes. As the target bacteria was introduced to the system, the FAM-labeled cDNA was instantly released to the solution, owing to the dissociation of FAM-cDNA from the streptavidin/biotin-TL43/FAM-cDNA complex causing a quenching of fluorescence polarization signals. A linear relationship was obtained between the changes in fluorescence signals in comparison with the target bacteria in the range from 10^2 to 10^6 cfu mL^{-1} (Figure 7C) along with the specificity test of the developed aptasensor (Figure 7D) [42].

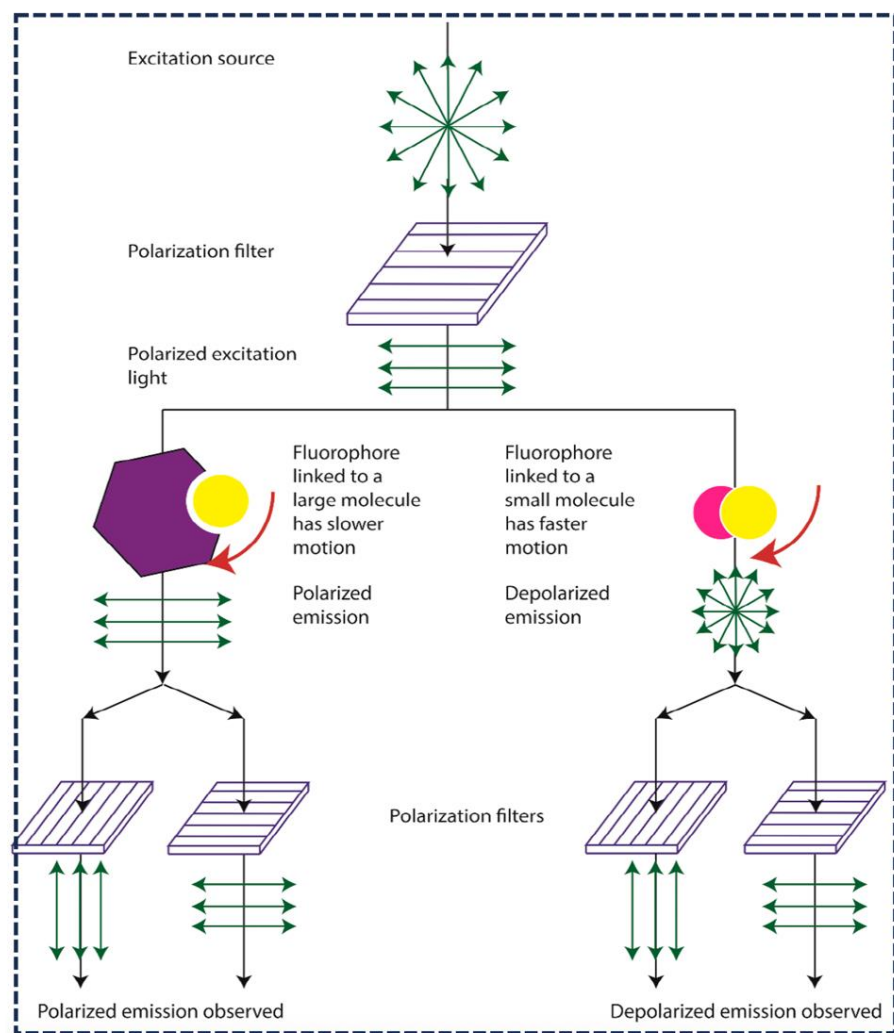


Figure 6. Schematic describing the principle of fluorescence measurement undergoing irradiation with plane-polarized light [40] Sensors 20, no. 24: 7132. <https://doi.org/10.3390/s20247132> © 2020 by the authors. Licensee MDPI, Basel, Switzerland. This article is an open access article distributed under the terms and conditions of the Creative Commons Attribution (CC BY).

Ye et al. [43] have worked on aflatoxin B1 (AFB1), which is one of the most toxic mycotoxins of the aflatoxins (AFs) that has shown teratogenic, mutagenic, and carcinogenic effects in humans and animals. Mycotoxins, in general, are released by various molds, posing great hazards on humans' and animals' health through food contamination or feed. Until now, over 300 kinds of mycotoxins have been identified and recognized, which amongst them aflatoxins are the most toxic ones, known as aflatoxin B1, B2, M1, M2, etc. Ye et al. [43] used an aptamer biosensor that was based on graphene oxide in a low-cost

high-sensitivity fluorescence polarization-assay format to detect AFB1, which is widely seen in cereal products such as rice and wheat. The aptamer was labelled with fluorescein amidite and was adsorbed on the surface of graphene oxide, forming aptamer–graphene oxide macromolecular complexes. Such conditions caused the system to have a high fluorescence polarization value due to limited local rotations of fluorophores. When AFB1 was introduced, aptamers were dissociated from the graphene surface and combined with AFB1, forming aptamer-AFB1 complexes. Changes in fluorescence polarization signals were observed and large changes in aptamers' molecular weight before and after the combination was observed. A linear relation within 0.05 to 5 nM of AFB1 was observed between changes in fluorescence polarization and the AFB1 concentration obtaining a detection limit of 0.05 nM with high specificity. It is important to highlight that the changes in fluorescence polarization widely depend on both fluorophore and receptor sizes. The larger the difference in their sizes, the more dominant the changes detected in fluorescence polarization will be due to the transition of fluorophore from free to bound states. However, since ligand size depends on the target chosen and is unchangeable, the only variable could be the size of the receptor or the ligand–receptor complex that may vary. This concept has been highlighted in a few publications on fluorescence polarization-based aptasensors by Samokhvalov et al. [44] Kang et al. [45], and Li et al. [46].

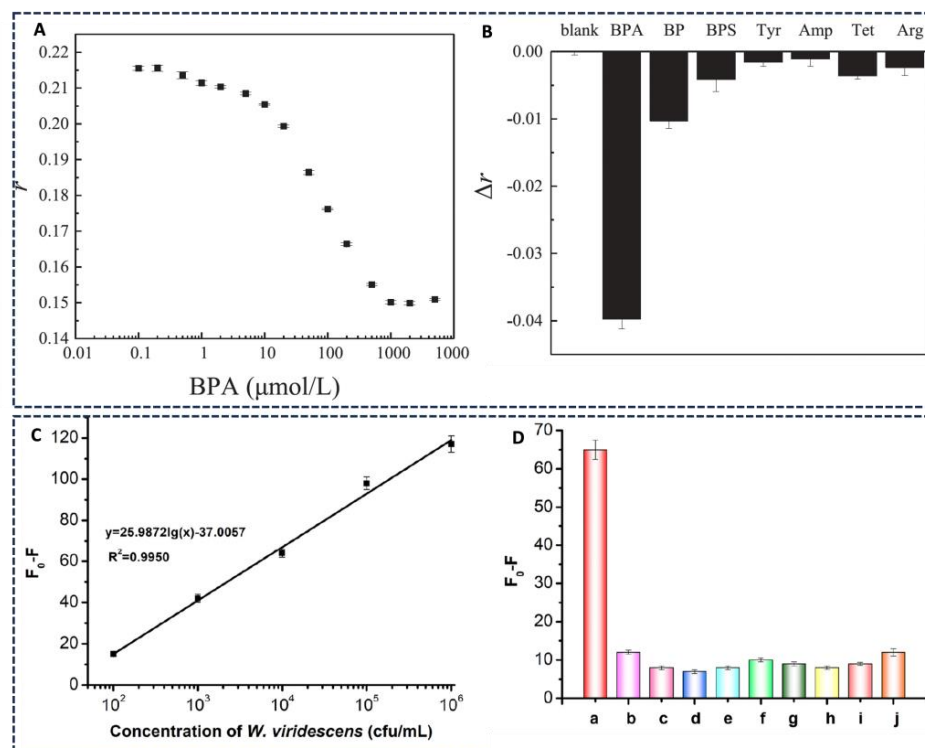


Figure 7. (A) Direct fluorescence polarization assay of BPA using aptamer probe BP35–22T-TMR. (Reprinted from [41] Copyright (2020), with permission from Elsevier.) (B) Selectivity of fluorescence polarization assay using BP35–22T-TMR for the detection of BPA. (Reprinted from [41], Copyright (2020), with permission from Elsevier). (C) A standard correlation curve plotted between the changes in fluorescent polarization (FP) and the concentration of *Weissella viridescens* with the help of constructed aptasensor ($F_0 - F = FP$ changed; where F_0 is the initial value and F being the FP value on target addition). (Reprinted from The Lancet, [42], Copyright (2022), with permission from Elsevier.) (D) Specificity tests of the developed aptasensors; shown in graph labelled as follows: (a) *Weissella viridescens*; (b) *Leuconostoc mesenteroides*; (c) *Lactobacillus plantarum*; (d) *Pediococcus pentosaceus*; (e) *Lactobacillus brevis*; (f) *Lactobacillus sakei*; (g) *Staphylococcus aureus*; (h) *Salmonella typhimurium*; (i) *Escherichia coli O157:H7*; (j) Dead *W. viridescens*. (Reprinted from The Lancet, [42], Copyright (2022), with permission from Elsevier).

3.1.3. Wavelength-Shifting Aptasensors

Aptasensor-based wavelength-shifting detection techniques are an interesting avenue that have been explored by a few researchers for their rapid and sensitive detection. Various versatile configurations using different optical techniques that optimize sensor performance have been explored. While various trends in the design of wavelength-based optical fiber biosensors have been constructed [47], Park et al. [48] have leveraged the progress in silicon-based resonator devices to demonstrate a label-free DNA aptamer sensor. This sensor is based on the use of a silicon microring resonator for the detection of the immunoglobulin E (IgE) antibody as well as thrombin. The resonators, that are essentially refractive index-based sensors, allow for light to propagate in the form of circulating waveguide modes resulting from the total internal reflection of light between the high- and low-refractive index media. Park et al. utilized the fact that resonator wavelength shifts are in direct proportion to the mass change in analytes bound to the surface (Figure 8A) [48]. Silicon-based microring resonators were designed in order to demonstrate the use of aptamer-modified silicon microring resonators over a broad range of antigen concentrations. These authors presented an experimental detection limit of 33 pM and 1.4 nM for IgE and thrombin, respectively (Figure 8B,C). They also demonstrated multiplexing using a mixed solution of IgE and thrombin. This aptamer-based silicon micro ring resonator technology has the potential for point-of-care applications. The progress in the field of such silicon-based optoelectronic devices was also reviewed recently by Mitin et al. (2019) [49]. James Yang (2005) [50], on the other hand, molecularly engineered aptamer probes for platelet-derived growth factor-biomarker protein detection. Labelled at each end with one pyrene, the fluorescence emission from the aptamer is shifted from 400 nm (pyrene monomer, life time: 5 ns) to 485 nm (pyrene excimer, life time: 40 ns) upon binding with platelet-derived growth factor as shown in Figure 8. This wavelength shift from monomer to excimer emission is caused by aptamer-conformation rearrangement upon target binding. Such lifetime-based measurements engineered with light-switching excimer aptamer probes for protein monitoring hold great potential for biomedical studies. In addition, this design arrangement solved significant background signal problems in complex biological samples.

3.1.4. Multi-Analyte Detection

The simultaneous detection of several biomarkers within complex biological fluids is of vital importance. Since biological fluids consist of blood, serum, urine, etc., that may interfere with single analyte detection in real samples, designing and engineering aptasensors with the ability to target multiple analytes could save time and cost, and could further provide detailed information on array of biotargets [51–53]. Until now, very few multi-analyte aptasensor studies have been introduced, with the most popular being optical and electrochemical detection techniques, of which some of the important aspects will be highlighted.

In 2014, Saberian-Borujeni et al. [12] gave a detailed discussion on many advantages and notable successes in the use of aptamer-based nanosensors for multi-analyte detection. When different aptamers, each capable of binding to a particular analyte, are bound to a surface or nanoparticle, it is necessary to ensure that the aptamers are separated by distances that ensure there is little interference between neighboring aptamers when they undergo confirmational changes due to the binding of analytes. As surveyed by Saberian-Borujeni et al. in 2014 [12], McCauley et al. in 2003 [54] demonstrated simultaneous detection on a chip for inosine monophosphate dehydrogenase, thrombin, and growth factors for fibroblast and vascular endothelial tissue. Functionalization of the aptamer was performed using a biotin group and a fluorescein group at the 5' and 3' ends of the aptamer, respectively. As shown in Figure 9A, a fluorescence change was detected upon aptamer-analyte binding on the chip. In this multi-analyte chip—with different aptamers immobilized on specific positions on the chips—each analyte was detected by knowing the positions of different aptamers on the surface of each chip. In another representative approach to multi-analyte detection reported by Cho et al. (2006) [55], fluorescence aptamer-

based array was designed by labeling the analytes; specifically, in this approach lysozyme and ricin were labeled by RNA aptamers, and IgE and thrombin by DNA aptamers. In this sensor chip, the aptamers were modified by biotin for immobilization on a specific region of an avidin-coated glass slide, which was exposed to a solution containing the analytes. In this study, lysozyme was detected in the picomolar concentration range; in addition, ricin, IgE, and thrombin were detected in the nanomolar concentration range.

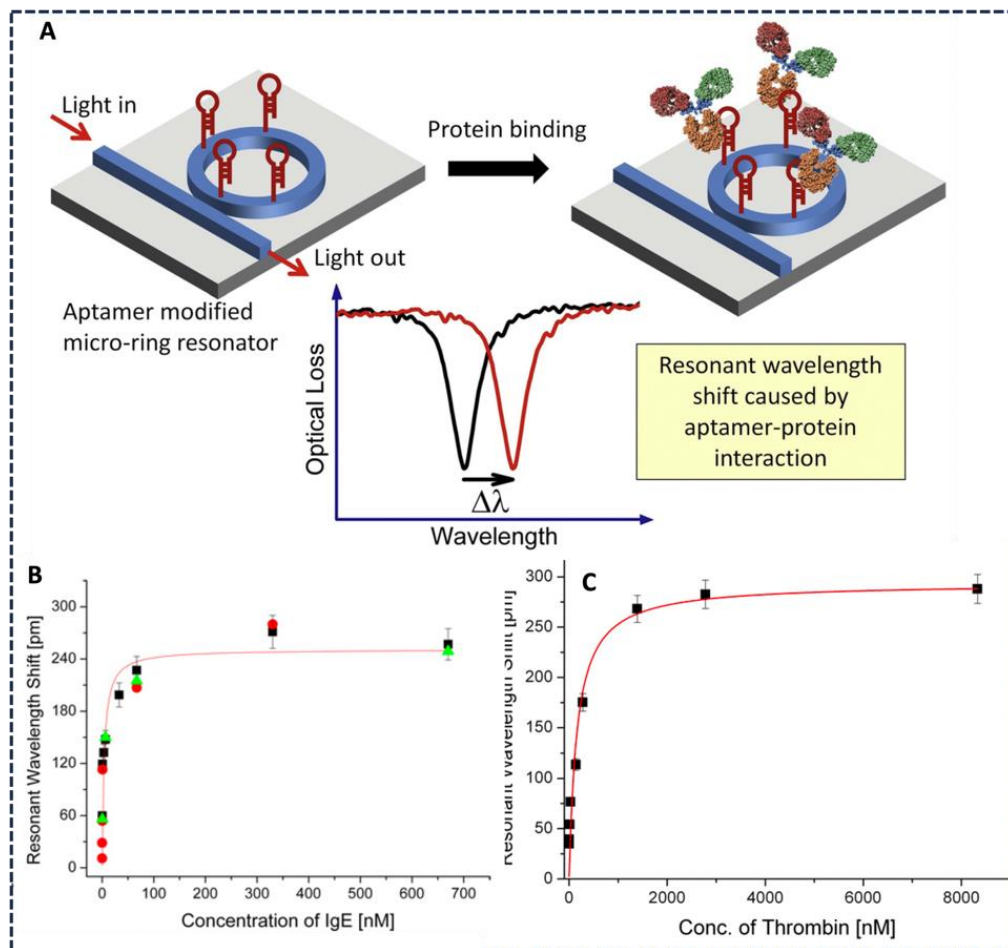


Figure 8. (A) Schematic showing microring resonator principle long with an optical loss spectrum. (B) Binding curve for IgE detection with silicon microring modified with anti-IgE aptamer showing resonant wavelength shift versus different concentration of IgE solution. (C) Binding curve for thrombin detection with anti-thrombin aptamer showing resonant wavelength shift versus different concentration of thrombin solution [48]. (Reprinted from Label-free aptamer sensor based on silicon microring resonators, [48], Copyright (2013), with permission from Elsevier).

In a related study by Kirby et al. (2004) [56], ricin and lysozyme were detected using a single chip and a bead-based aptasensor. In this study biotinylated aptamers were immobilized on streptavidin agarose beads which were loaded into the wells of a chip. The labeled analytes were introduced into the wells where the aptamer-analyte complex was detected via the fluorescent labels. Interestingly, these aptamer chips could be denatured and reused many times on the same chip as compared to protein-based arrays. The electronic tongue experimental setup used for the detection is shown in Figure 9B. For a more comprehensive treatment of aptamer-based multi-analyte detection, the reader is referred to the review by Saberian-Borujeni et al. (2014) [12].

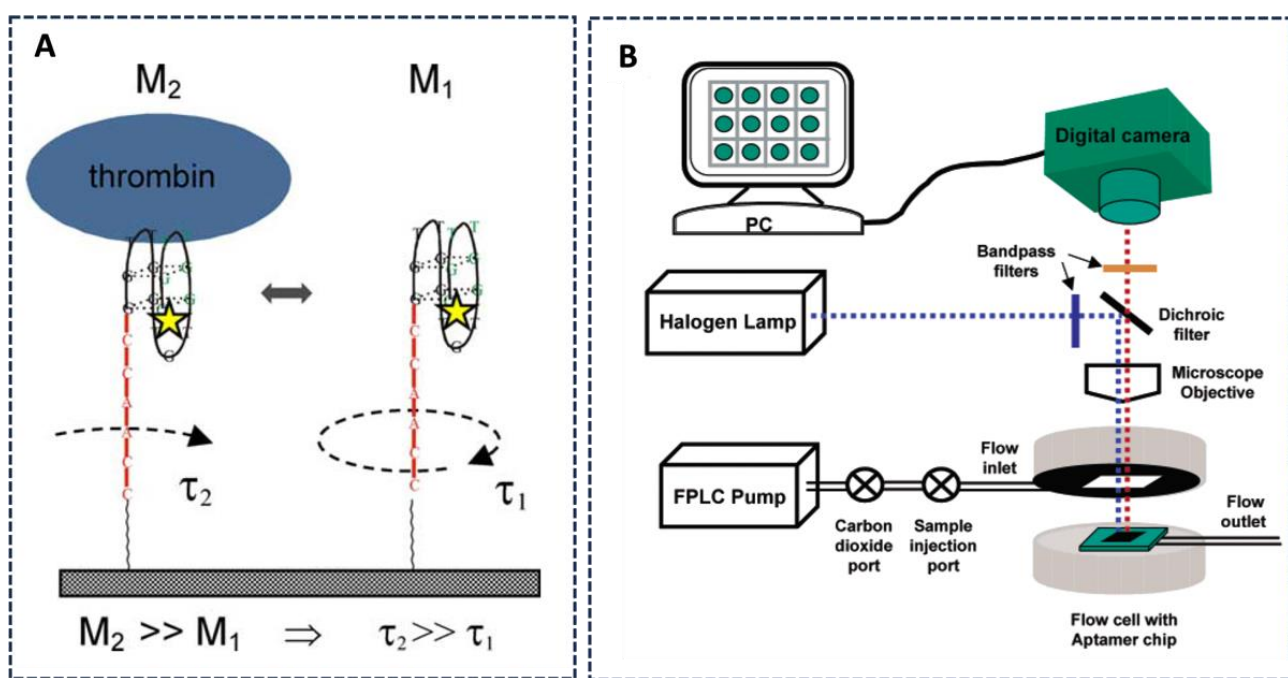


Figure 9. (A) Thrombin binding effects on the mobility of fluorophore for fluorescence polarization anisotropy measurements. (Reprinted from [54] Copyright (2003), with permission from Elsevier). (B) The electronic tongue setup employed contained a system comprising of a fluid delivery system; fluorescence microscope; digital camera; a flow cell, in which the aptamer chip would be loaded; and a computer for data computations. (Reprinted with permission from [56] Copyright (2004) American Chemical Society).

3.1.5. Colorimetric Bioassay

Another domain that has been paid attention to recently to develop is colorimetric bioassay formats. These methods are considered efficient and simpler in preparation, especially for point-of-care diagnostics and on-site testing [57,58]. Typically, many colorimetric biosensors use Au nanoparticles and detect targets using color change with the aid of the naked eye or simpler instrumentation methods. The negatively charged Au nanoparticles bind noncovalently to the electropositive amino DNA aptamer bases as demonstrated in Figure 10A [15]. Shaban and Kim (2021) [59] have recently surveyed progresses in colorimetric sensing based on the use of aptamers and assemblies of nanoparticles that manifest surface plasmon resonances (SPRs), leading to an emission color that depends on the separation distances of the assembled nanoparticles. In many of these colorimetric detection schemes Au nanoparticles are used for color-change-based detection. One example is nanoassemblies of AuNPs functionalized with aptamers for constructing aptasensors. Indeed, the color of AuNPs assemblies is extremely sensitive to their dispersion and aggregation in a solution as a result of SPR shifts due to changes in interparticle separations. In one application, Taghdisi et al. (2015) [60] discussed such an aptasensor for the selective, sensitive, and fast detection of lead (II) based on polyethyleneimine and gold nanoparticles. In a related application, Priyadarshni et al. (2018) [61] have discussed nanorods on paper for colorimetric detection and the estimation of arsenic contamination in groundwater. As another example, Li and Rothberg (2004) [62] have reported on colorimetric detection of DNA sequences based on electrostatic interactions with unmodified gold nanoparticles. Moreover, Guo et al. (2017) [36] have studied DNA nanopores functionalized with aptamers and cell-penetrating peptides for tumor cell recognition. In addition, Guo et al. (2015) [63] have discussed strategies for enhancing the sensitivity of plasmonic nanosensors.

In some cases, magnetic nanoparticles have also been used as a nano-assembling template for bioassays either on their own, or sometimes combined with other nanostruc-

tures where they can easily be separated from the solution with the aid of an external magnetic field. Priyadarshni et al. [61] showed the effects after functionalization with an ATP aptamer; the catalytic activity of the Fe_3O_4 nanoparticles was increased significantly, which caused the colorless TMB to turn into blue TMB. Upon the addition of an ATP target, it bound with the aptamer, which departed from the surface of Fe_3O_4 . This caused a decrease in activity and a detection limit of 0.09M. Another method to replace antibodies with aptamers in the ELISA protocol has attracted interest, especially for food borne pathogens. Wei et al. [64] described a photothermal multicolor bioassay from an ELISA-modified aptamer for the detection of prostate-specific antigens (Figure 10B). In this arrangement, a Fe_3O_4 graphene oxide nanoparticle functionalized with DNA served as the signal producer for assaying the PSA. A limit of detection of 0.15 and 0.31 ng/mL for colorimetric and photothermal assays were achieved.

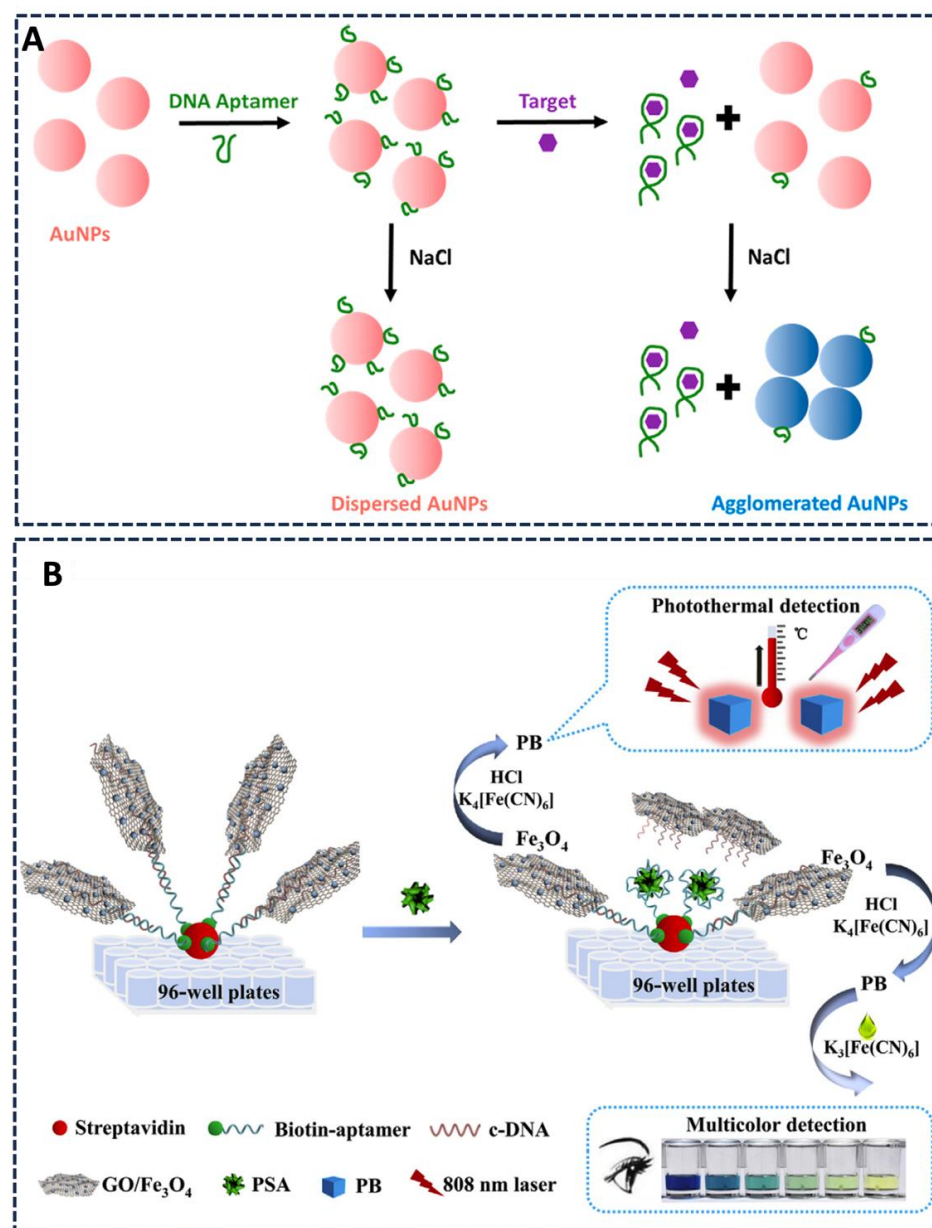


Figure 10. (A) A conceptual model of colorimetric sensor. (Reprinted (adapted) with permission from [15] Copyright (2018) American Chemical Society.) (B) Schematic illustrations of sensing platforms based on multicolor and photothermal dual-readout. (Reprinted from [65] Copyright (2019), with permission from Elsevier).

3.2. Electrochemical Aptasensors

Electrochemical biosensors have been utilized in various arenas to detect analytes via immunoassays. They have received special attention compared to other types of sensors and are increasingly gaining interest due to their lower costs, ease of scalable detection signal readout modalities, device miniaturization, faster response times, portability, and major progress in microelectronic fabrication techniques [65,66]. Aptamer-based electrochemical biosensors have gained popularity in analytical chemistry as well. In some cases, nanomaterials are integrated into the sensor to enhance the surface area of electrodes along with catalyst redox reactions. While the first electrochemical aptasensor constructed in 2004 by Ikebukuro et al. [67] was based on a glucose dehydrogenase-labeled aptamer with an amperometric-based biosensor, some of the recent developments include carbon nanomaterials, MoS₂, graphene oxide, metallic nanoparticles, and porous platinum surfaces, which have gained special attention for the construction of electrochemical aptasensors [68].

3.2.1. Molybdenum Disulfide Nanosheet-Based Sensors

Most recently, molybdenum disulfide (MoS₂) nanosheets were utilized to make electrochemical biosensors with good sensitivity [69]. Owing to their unique properties and graphene-like structures with an outstanding electron mobility and large surface-to-volume ratios, they have attracted an increasing number of scientists' interests. MoS₂ is an interesting semiconducting material with an indirect-to-direct bandgap transition from 1.2 to 1.9 eV that depends on its thickness. Furthermore, MoS₂ nanosheets have demonstrated the ability to adsorb single-stranded DNA; hence, they can be utilized for the construction of electrochemical sensors efficiently for highly sensitive detection [70]. In 2018, Qiao et al. [71] developed an electrochemical sensing platform for the detection of cardiac troponin I (cTnI), which is a biomarker for the early diagnosis of acute myocardial infarction based on aptamer-MoS₂ nanoconjugates. MoS₂ nanosheets were immobilized on the electrode surface at first, followed by incubation in an aptamer mixture in order to build an aptasensor. In the absence of target cTnI, the aptamer-based probe was mainly in the unfolded or flexible state and lay on MoS₂ nanosheets naturally, as shown in Figure 11A. Upon the addition of cTnI to the aptamer-MoS₂ nanosheets into the sensing system, the aptamer specifically bound to the target and the detection of cTnI was realized based on impedance changes. A detection limit of 0.95 pM was achieved with a linear range for cTnI detection from 10 pM to 1.0 μM, as shown in Figure 11B. In another recent study in 2022 by Gao et al. [72], electrochemical aptamer sensing of ochratoxin A (OTA), one of the most toxic mycotoxins in food, via cascaded amplifications was achieved using NiCo₂S₄ nanoparticle-dispersed MoS₂ nanosheets. The sensor was based on the DNAAzyme-powered DNA walker along with hybridization chain reaction-amplification strategies. A nanocomposite (NiCo₂S₄-MoS₂) was used as an electrocatalyst along with significant signal amplifications, leading to enhanced sensitivity for OTA and a detection limit of 0.42 pg mL⁻¹. The nanocomposite collected a large volume of signal probes in order to obtain a constant difference in voltammetry responses. As shown in Figure 11C, the peak current enhanced gradually with increasing the concentrations of OTA from 0 to 1 ng mL⁻¹ with good sensitivity. Another interesting nanocomposite based on DNA aptamer-graphene-MoS₂ was constructed by Kim et al. in 2022 [73] for the fabrication of a Middle East respiratory syndrome coronavirus (MERS-CoV) MERS-nanovesicle (NV) biosensor based on electrochemical and surface-enhanced Raman spectroscopy (SERS). This MERS-NV was specifically designed for binding to the spike protein and was prepared using the SELEX technique. The prepared aptamer was first connected to the DNA three-way junction possessing three arms that could connect to the three individual functional groups including the aptamer, the reporter, and the linker. The assembled DNA aptamer was immobilized on a graphene oxide-MoS₂ structure and could detect MERS-NVs with a limit of detection 0.645 pg mL⁻¹ (Figure 11D).

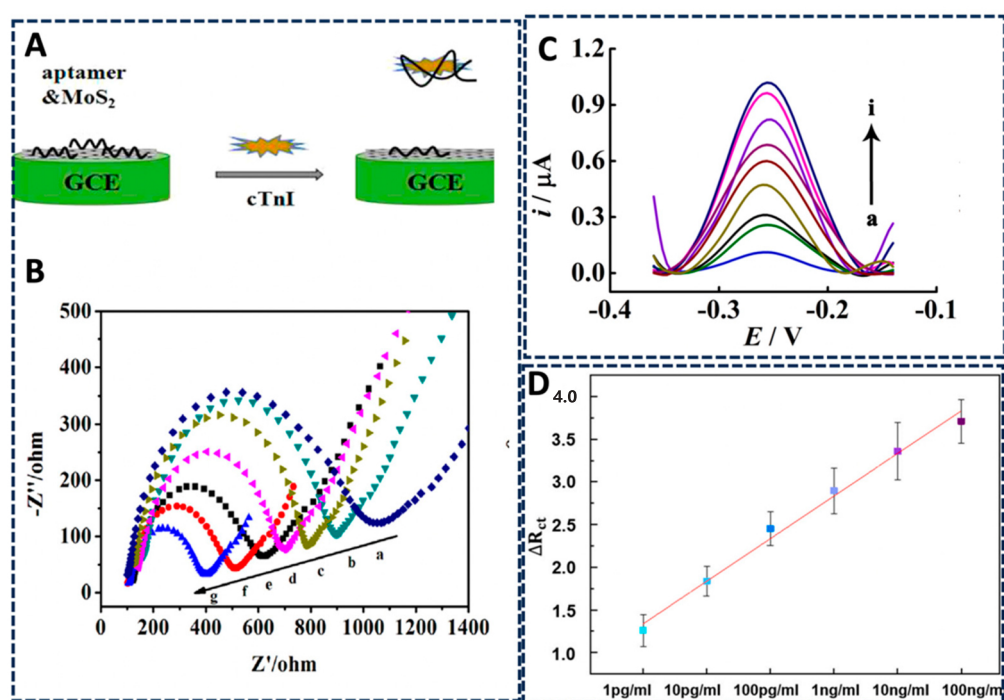


Figure 11. (A) The scheme of detection of cTnI by the aptasensor based on MoS₂ nanosheets [71]. (B) Nyquist plots of the aptasensor based on MoS₂ nanosheets with cTnI ranging at 0, 10.0 pM, 100.0 pM, 1.0 nM, 10.0 nM, 0.1 μ M, and 1.0 μ M concentrations [71]. (Reprinted from [71] Copyright (2018), with permission from Elsevier.) (C) Square wave voltammetry current curves for the detection of OTA at different concentrations from 0 pg mL^{-1} to 1 ng mL^{-1} [72]. (Reprinted from [72] Copyright (2022), with permission from Elsevier.) (D) Linear curve of MERS-NV concentrations ranging from 1 pg mL^{-1} to 100 ng mL^{-1} [73]. (Reprinted from [73] Copyright (2022), with permission from Elsevier).

3.2.2. Graphene Oxide Aptasensors

In addition to MoS₂ and its composites, several carbon-based nanomaterials such as graphene oxide, carbon nanotubes, and graphene quantum dots have been used extensively in the fabrication of electrochemical aptasensors [74]. Farid et al. [75] developed a graphene monolayer-based FET-like structure to detect interferon-gamma, which is linked with tuberculosis susceptibility. A mono-graphene layer was used as a conducting substrate between the source and drain electrodes as shown in Figure 12A. A change in charge distribution is detected upon target addition through an increase in electron-transfer efficiency measured by current–voltage measurements. A detection limit of 83 pM was achieved and a device transfer curve was shown upon target addition, ranging from 0 nM to 100 μ M as shown in Figure 12A, causing a dynamic increase in current. Another graphene-based FET-like electrochemical nano-biosensor was fabricated by Mukherjee et al. [76] to detect ultra-low concentrations of adenosine triphosphate (ATP). The sensor appears to be highly sensitive to ATP concentrations from nano to micromolar levels, with a detection limit of as low as 10 pM. In a related study, Datta et al. [24] detected adenosine monophosphate (AMP) using a graphene-based field effect transistor electrochemical nanobiosensor. The sensor appears to be nonlinear in nature but sensitive in the picomolar to nanomolar range with an ATP-detection limit of 10 pM.

Appaturi et al. [77], in 2020, fabricated an aptasensor based on carbon nanotubes for *Salmonella enterica* detection. The developed nanocomposite was drop-casted onto the carbon electrode and modified with the DNA aptamer as shown in Figure 12B. The synthesized aptasensor was then used to detect bacteria by using the differential pulse voltammetry technique. The complete working electrode demonstrated a wide linear dynamic range from 10^1 to 10^8 cfu mL^{-1} with a limit of detection of 10^1 cfu mL^{-1} . The sensor

exhibited selectivity and could successfully distinguish *Salmonella* from non-*Salmonella* cells. Similarly, Muniandy et al. [78] have also demonstrated an electrochemical biosensor, using reduced-graphene oxide nanomaterial for the detection of foodborne pathogens. He developed a reduced graphene oxide-azophloxine (AP) nanocomposite aptasensor where the AP dye was used as an electroactive indicator for redox reactions. A detection limit of 10^1 cfu mL^{-1} was achieved and a differential pulse voltammetry was employed for the detection of target pathogen *Salmonella*.

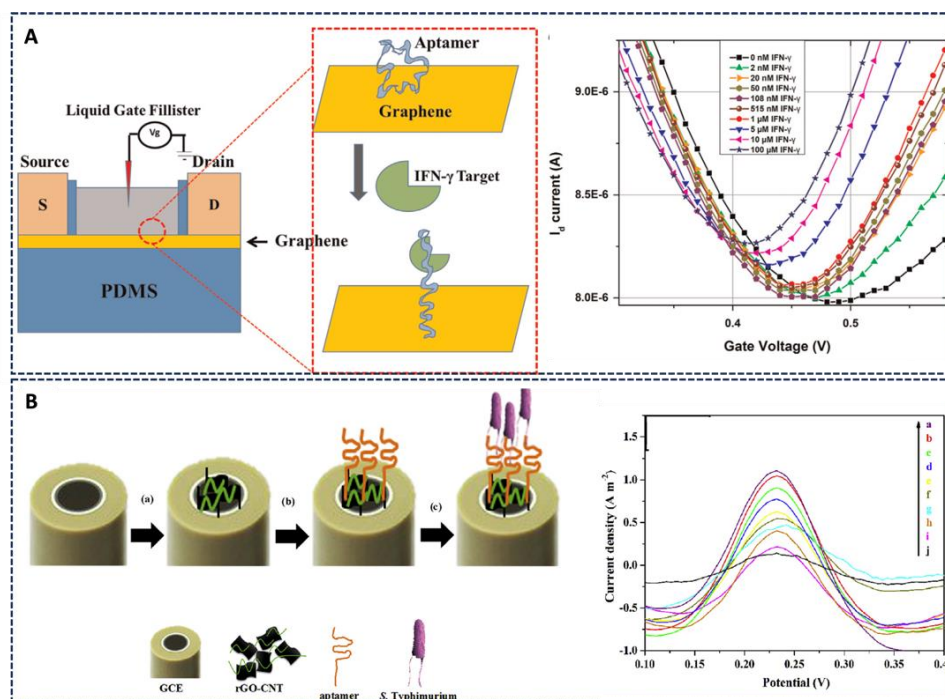


Figure 12. (A) Schematic illustration of graphene-based electrochemical biosensor. Graph on right indicates device transfer curves on IFN- γ target addition with concentrations varying from 0 nM to 100 μM [75] [Reprinted from [75] Copyright (2015), with permission from Elsevier]. (B) A schematic illustration of the various modification processes of substrate. Figure on right showing aptasensors sensitivity test on various *S. Typhimurium* concentrations as shown from (a) ssDNA/rGO-CNT/GCE, (b–i) 10^8 cfu mL^{-1} – 10^1 cfu mL^{-1} , and (j) rGO-CNT/GCE [77]. (Reprinted from [77] Copyright (2020), with permission from Elsevier).

3.2.3. Metallic Nanoparticles

In some cases, metallic nanoparticles are also inclined to be combined in with catalytic procedures due to high surface energies, especially 3D nanomaterials due to their high surface–volume ratio [79]. Tian et al. [80] developed a dual aptamer-based electrochemical sensor to detect SARS-CoV-2 nucleocapsid proteins with co-catalysis of the nanomaterials Au@Pt/MIL-53(Al), DNAzyme, and horseradish peroxidase. This nanoconstruct was used for the amplification of an aptasensor signal via co-catalyzing the oxidation of hydroquinone in the presence of hydrogen peroxide. The aptamer–protein–nanoprobe sandwich electrochemical detection system demonstrated a limit of detection of 8.33 pg mL^{-1} along with dynamic range of from 0.025 to 50 ng mL^{-1} for 2019-nCoV-NP, as shown in Figure 13A. Karimi et al. [81] reported a 27-base DNA aptamer for the detection of adenosine-5'-triphosphate (ATP) via firefly luciferase activity and gold nanoparticles (AuNP). As seen in Figure 13B, the application of ATP increased firefly luciferase activity, which improved detection limits up to $5 \mu\text{M}$ for ATP. In another study, Qi et al. [82] reported a SERS biosensor to detect *S. aureus*, which was based on teicoplanin (Tcp)-functionalized gold-coated magnet ($\text{Fe}_3\text{O}_4@\text{Au-Tcp}$) nanoparticles as capture probes and *S. aureus*-specific aptamer-functionalized silver-coated gold ($\text{Au}@\text{Ag-DTNB-Apt}$) nanoparticles as signal

probes. Based on the dual recognition capacity using Tcp for Gram-positive bacteria and specificity of aptamer for *S. aureus*, the designed SERS biosensor was ultrasensitive and specific. A dynamic linear range of 7.6×10^1 – 7.6×10^7 CFU mL^{-1} along with a detection limit of 1.09 CFU mL^{-1} was achieved within 50 min without interference by other bacteria. Several nanoparticle-based aptasensors have been reported for cancer diagnosis. For instance, Wang et al. [83] developed a TiO_2/CdTe heterostructure conjugated to aptamer AS1411 for MCF-7 cell detection. This aptasensor demonstrated excellent specificity and sensitivity for MCF-7 cell concentrations ranging from 1×10^3 to 1×10^5 cells mL^{-1} (Figure 13C). Liu et al. [84] developed an aptamer–nanoparticle strip biosensor (ANSB) for the fast, precise, delicate, and low-cost detection of circulating tumor cells. In this study, Ramos cells were utilized as a standard. The designed ANSB was observed to detect approximately 4000 Ramos cells without instrumentation, while using a portable strip reader around 800 Ramos cells that were detected within 15 minutes. In another study reported by Yang et al. [85], a photoelectrochemical sensor was developed using $\text{C}_60@\text{C}_3\text{N}_4$ nanocomposites as a quencher and Au nanoparticles (depAu) decorated perylene tetracarboxylic acid (PTCA) for detecting various concentrations of thrombin in a linear range from 10 fM to 10 nM and with an LOD of 1.5 fM (Figure 13D). In this study, PTCA and depAu produced an extremely high initial photocurrent, which helped with the biosensing. Subsequently, the assembly of $\text{C}_60@\text{C}_3\text{N}_4$ nanocomposites on the electrodes via the typical sandwich reaction resulted in a decrease in the photocurrent.

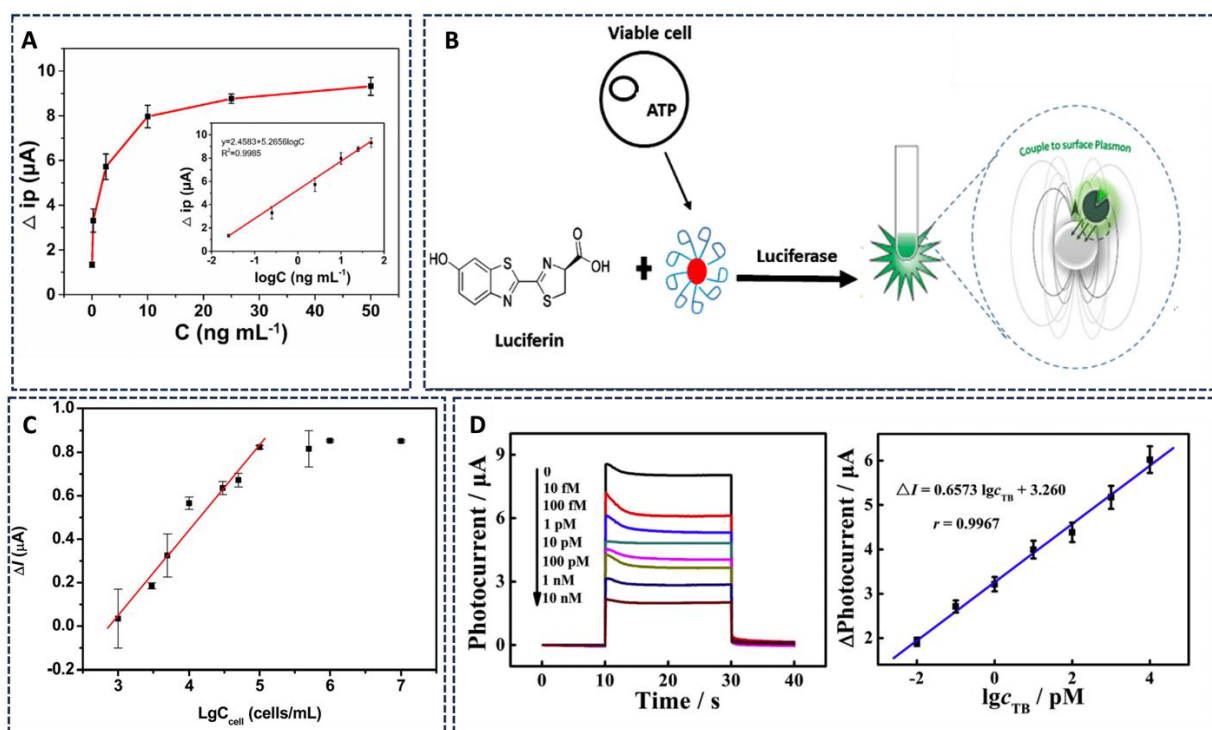


Figure 13. (A) Differential pulse voltammetry of the aptasensor for the detection of 2019-nCoV–NP with various concentrations from 0 – 50 ng mL^{-1} [80]. (Reprinted from [80], Copyright (2021), with permission from Elsevier.) (B) Schematic illustration showing cell viability detection by ATP [81] © 2022 by the authors. Licensee MDPI, Basel, Switzerland. This article is an open access article distributed under the terms and conditions of the Creative Commons Attribution (CC BY) license (<https://creativecommons.org/licenses/by/4.0/>, accessed on 1 January 2021). (C) Photocurrent effects of AS1411-immobilized $\text{NaYF}_4:\text{Yb}, \text{Er}/\text{TiO}_2/\text{CdTe}$ electrodes on various MCF-7 cells concentrations [83]. (Reprinted with permission from [83] Copyright {2016} American Chemical Society.) (D) Photocurrent responses for various thrombin concentrations of the PEC aptasensor along with the subsequent corresponding calibration curve [85]. (Reprinted from [85], Copyright (2019), with permission from Elsevier).

3.2.4. Electrochemiluminescence-Based Sensors

Along with conventional electrochemical sensors, electrochemiluminescence (ECL)-based sensors are another efficient type of detection that combine the advantages of electrochemistry with the sensitivity of chemiluminescence. Some of these advantages include control over the position of light emission, which also helps with lowering background signal. Additionally, there is no requirement for an extra light source (Miao et al. Kurup et al.) [86,87]. An attribute of a good biosensor is excellent signal enhancement along with low detection limits. As shown in Figure 14A [87], nanomaterials can be used as electrode modifiers, nanocarriers, nanocatalysts, and luminophores in ECL. Wei et al. [88] developed a label-free ECL aptasensor based on CdS quantum dots (CdSQDs) loaded onto a metal organic framework (MOF) (CdSQDs@MOF) and triethanolamine modified on AuNPs (TEOA@AuNPs) as bi-co-reactants of a Ru(bpy)₃²⁺ ECL system for the detection of carcinoembryonic antigen. An LOD of 85 fg/mL and a linear range of 100 fg/mL to 10 ng/mL was achieved using this aptasensor (Figure 14B). In another study, Liu et al. [89] reported a g-C₃N₄-COOH/ZnSe nanocomposite for kanamycin detection. The g-C₃N₄-COOH/ZnSe substrate was incubated with aptamer DNA (NH₂-DNA), and further with a ferrocene-labeled quenching probe (Fc-DNA) as an electrochemiluminescence signal quencher. Absence of kanamycin resulted in effective quenching of the ECL signal, while presence of kanamycin enhanced the signal. This sensor exhibited an LOD of 0.7982 nM with a detection range of from 1.0 nM–100 μM (Figure 14C). Gao et al. [90] published a study on an ECL-based resonance energy transfer (ECL-RET) for sensitive detection of ochratoxin A (OTA). The sensing strategy was based on the significant spectral overlap between the ECL emission of CdTe QDs and the absorption spectrum of cyanine dye (Cy5) fluorophores. The developed biosensor demonstrated high specificity towards the target and had a wide detection range of 0.0005–50 ng mL⁻¹ along with an LOD of 0.17 pg mL⁻¹ (Figure 14D). Wang et al. [91] developed an ECL-RET-based aptasensor involving lanthanide ion-doped cadmium sulfide quantum dots (CdS:La QDs) with aptamer-conjugated AuNPs for thrombin and Hg²⁺ detection. High sensitivity with LODs at 3.00×10^{-13} mol L⁻¹ and 3.00×10^{-17} mol L⁻¹ for Hg²⁺ and thrombin, respectively, were demonstrated by this sensor.

3.2.5. Electrochemical Multi-Analyte Detection

Owing to all the advantages discussed earlier, electrochemical methods make up a versatile tool for multi-analyte biosensing. Designing biosensors that are capable of multiplexing two or more analytes' detection in a single readout stands out. Grabowska et al. [92] have presented a detailed analysis and categorization of various sensing modes using multi-label or multi-electrode approaches (Figure 15). The multi-label approach uses a single electrode to produce distinguishable electrochemical signals. Few multi-sensing approaches have been tried based on metal ions, quantum dots, redox labels, or enzyme labels using this approach [93]. On the other hand, the multi-electrode system consists of multiple sensing areas and is able to detect multiplexed analytes. Its most prominent feature includes low cost-per-test, high throughout, and operational convenience. Xiang et al. [94] have proposed a signal probe-based aptasensor for the detection of dual-analyte. The author used two different aptamer probes labeled with redox tags integrated into one DNA architecture to develop the signal probe. This system reduces any cross interference between the two aptamer probes by regulating their complementary positions, ensuring the same modifications conditions and equal stoichiometric ratios. Combined with gold nanoparticles signal amplification for the enhancement of detection sensitivity, using MUC1 and CEA as a model, disease-related biomarkers were simultaneously detected with high sensitivity and reproducibility. Pakchin et al. [95] have presented some recent advances in this domain. “Lab-on-a-chip” or, more recently, “organ-on-a-chip” systems that may have seemed fictional in the past are coming to reality due to the amalgamation of systems like multiplexed sensors or chip-based multi-sensing systems beneficial to both patients and clinicians.

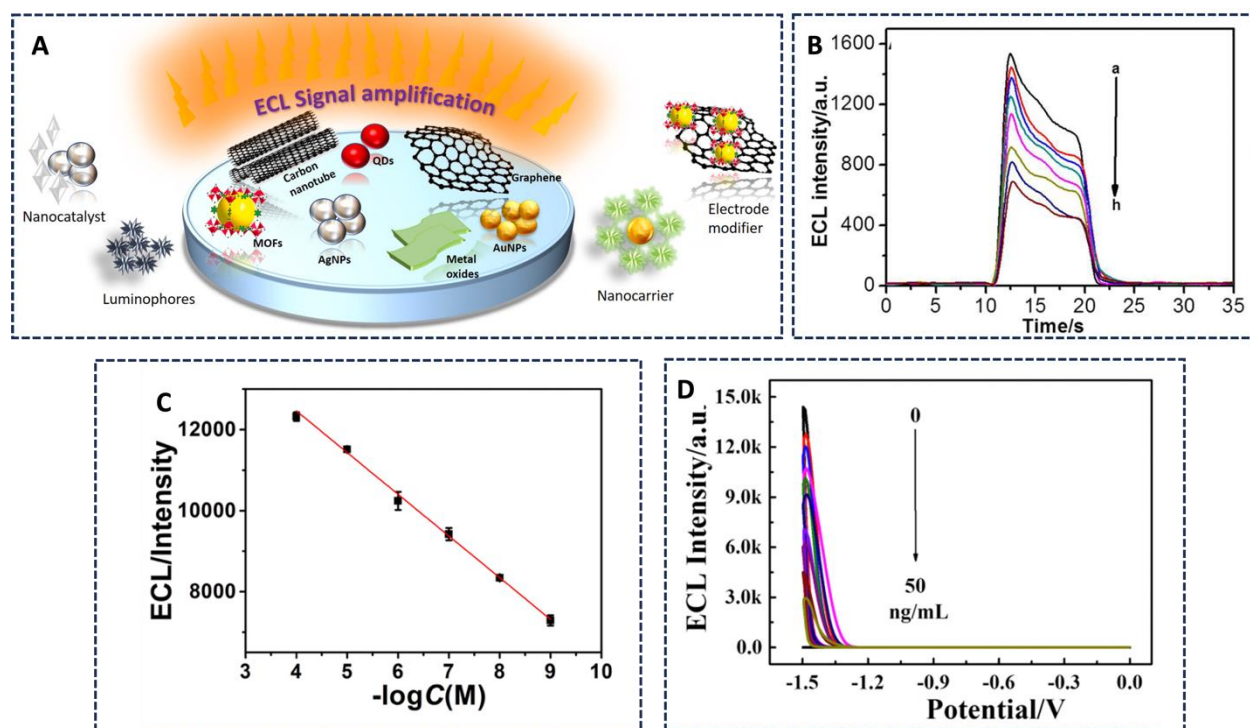


Figure 14. (A) Signal amplification strategies using several types of nanomaterials in ECL [87]. (Reprinted from [87], Copyright (2022), with permission from Elsevier.) (B) ECL response of the proposed aptasensor to the concentrations of CEA ranging from a) 100 fg mL^{-1} to h) 10 ng mL^{-1} [88]. (Reprinted from [88], Copyright (2022), with permission from Elsevier.) (C) Aptasensor calibration curve for various kanamycin concentrations ranging from 1.0 nM to $100 \mu\text{M}$ [89]. (Reprinted from [89], Copyright (2022), with permission from Elsevier.) (D) ECL response with various target concentrations from 0 to 50 ng mL^{-1} [90]. (Reprinted from [90], Copyright (2019), with permission from Elsevier).

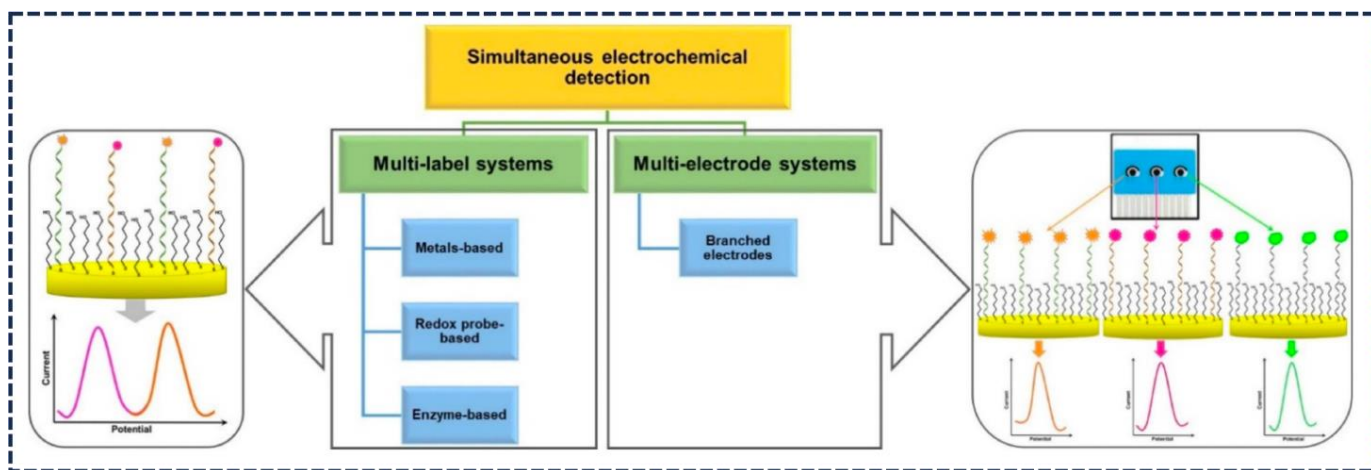


Figure 15. Simultaneous detection of multiple analytes using multi-label and multi-electrode electrochemical aptasensors [92] © 2021 by the authors. Licensee MDPI, Basel, Switzerland. This article is an open access article distributed under the terms and conditions of the Creative Commons Attribution (CC BY) license (<https://creativecommons.org/licenses/by/4.0/>, accessed on 1 January 2021).

4. Conclusions and Future Prospects of Aptasensors

An important comparison to realize between various aptasensor platforms is their limits of detection; however, this limit is impacted deeply by the inherent affinity of the

aptamer to the target, along with the sensitivity of the sensor platform that is being employed. An interesting correlation between the aptamer dissociation constant (K_d) and the limit of detection (LOD) was demonstrated by Akki et al. [15], showing a linear regression between the two quantities and demonstrating a lower K_d (higher binding affinity) yielding to a lower LOD (employing more sensitive sensors). In general, fluorescent aptasensors, FRET-based sensors, colorimetric sensors, etc., that are based on optical detection need to be labeled, are more prone to interference from colored or turbid samples, may contain more background fluorescence that increases their complexity and cost, and demonstrate poorer LODs as compared to electrochemical sensors. The electrochemical sensors with the lowest LODs can also be reused in many cases upon regeneration of the electrode surface. However, despite better LODs, electrochemical sensors do require a specific use of instrumentation for their functioning, for example, power source, potentiostat, etc. They often involve the immobilization of aptamers onto electrodes that reduce the aptamer's binding affinity, hence affecting sensor sensitivity. The electrochemical sensors with the lowest LODs, in most cases, involve complex fabrication details such as incorporating nanoparticles and polymer films. Table 1 summarizes the key signal transduction and response mechanisms for a clear comparison, including the detection limits of the discussed aptasensors.

Although remarkable progress have been made in the field of aptamer-based sensors, there are still some ongoing challenges and limitations to address. For instance, aptasensors for small organics, such as sensors for environmentally relevant concentrations in natural matrices, still appear to face selectivity and sensitivity challenges. To overcome this, they have to go through commercialization challenges including portability, production cost, stability, robustness, etc. Similarly, commercially available aptasensors for such organic pollutants are yet to be realized. Hence, new efforts are needed to develop aptasensors that are highly selective and sensitive in both free and surface state bounds.

In some cases, researchers have highlighted DNA aptamers when exposed to real environments, such as a complex biological medium. These DNA aptamers have demonstrated the detection of small molecule analytes with an affinity as low as 10 pM. Shayesteh et al. reported an aptasensor for the qualitative detection of kanamycin in human serum at a minimum concentration of 15 nM [96]. Aptamer-based sensors have been observed to exhibit low background signal and high specificity for small molecule analytes. In another study by Raouafi et al., a potentio-amperometric aptasensor was reported for the detection of prostate-specific antigen (PSA) [97]. This sensor was tested in human blood sera and showed around 100% recovery. Liquid biopsy, which focuses on the detection of circulating targets in complex matrices such blood, serum, urine, saliva, or semen, have shed light on the importance of aptamer-based sensors in this area. Li et al. designed an aptamer-based superparamagnetic complex for detecting exosomes in urine with an LOD of approximately 100 particles/ μ L [98].

However, the hardware utilized for aptasensors for multi-analyte sensing appears to be bulky and requires sophisticated instrumentation. While this is such an important arena to explore, point-of-care usage and portable life-supporting devices for daily usage are much needed for these biological readouts. A sensing system to monitor the personalized disease conditions of each individual on personal devices and smart phones are imaginable for monitoring key biofunctions. A few personalized cell-based therapies have already been put into practice; for example, Dendreon Corporation (Saturn Way Seal Beach, CA, USA) [99] developed an immunotherapy for cancer patients. In spite of the many advances in the field of aptasensors, due to a poor knowledge of surface immobilization technologies for aptamers, important additions in the diagnostic and analytical workbox need to be realized for this to become the real world tool, such as combinations of aptamers with novel nanomaterials, designing aptasensors for simultaneous multiple-target detection, analyzing real-time spiked samples and calculating the recoveries, focusing more efforts on the screening of aptamers that show high specificity and affinity. Lastly, in the future, researchers should not only pay keen attention to laboratory investigations; a major portion

needs to be dedicated to the commercialization of aptasensors that can achieve *in situ* detection efficiently.

Table 1. Summary of key signal transduction and response mechanisms including the detection limits of some of the discussed aptasensors (abbreviations: aggregation-induced emission fluorogen (AIEgens), gold nanoparticle (Au NP), quantum dot (QD), surface-enhanced Raman spectroscopy (SERS), field effect transistor (FET), electrochemical impedance spectroscopy (EIS), NA= not available).

Transduction Type	Target	Substances	Dynamic Range	LOD	References
Fluorescence	Intracellular IFN- γ	AIEgen: TPEN3 aptamer	0–10,000 pg mL ⁻¹	2 pg mL ⁻¹	[33]
Fluorescence	Liver cancer cells	Graphene oxide-based DNA nanomaterial	DSAI: 0.25–1 × 10 ⁻⁶ M	NA	[34]
Fluorescence	Nucleolin in living cells	Aptamer hairpin and DNAzyme	NA	1.8 pM	[35]
Fluorescence	Calcium ions	QD and Au NP	NA	3.77 pM	[38]
Fluorescence polarization	Bisphenol A (BPA)	Tetramethylrhodamine (TMR)	NA	0.5 μmol L ⁻¹	[41]
Fluorescence polarization	<i>Weissella viridescens</i> <td>TL43 aptamer</td> <td>10² to 10⁶ cfu mL⁻¹</td> <td>80 cfu mL⁻¹</td> <td>[42]</td>	TL43 aptamer	10 ² to 10 ⁶ cfu mL ⁻¹	80 cfu mL ⁻¹	[42]
Fluorescence polarization	Aflatoxin B1 (AFB1)	Graphene oxide	0.05 to 5 nM	0.05 nM	[43]
Refractive index-based sensors	Immunoglobulin E (IgE) and thrombin	Silicon-based resonator	0.27 nM to 0.5 M IgE; 1.4 nM to 8.1 M thrombin	33 pM: IgE; 1.4 nM thrombin	[48]
Fluorescence	Platelet-derived growth factor-biomarker protein detection.	Light-switching excimer aptamer probes	0–40 nM	NA	[50]
Fluorescence aptamer-based	Lysozyme, ricin, IgE, and thrombin	Aptamers modified by biotin on an avidin-coated glass slide	NA	5 pM lysozyme; 0.5 nM ricin; 0.01 nM IgE; 5 nM thrombin	[55]
Fluorescent	Protein analytes	Streptavidin agarose bead-based aptasensor		320 ng mL ⁻¹	[56]
Colorimetric	adenosine triphosphate (ATP)	Magnetic Fe ₃ O ₄ nanoparticles	NA	0.09 M	[61]
Colorimetric	Prostate-specific antigen	Fe ₃ O ₄ graphene oxide nanoparticles functionalized with DNA	NA	0.31 ng mL ⁻¹	[64]
Electrochemical	Cardiac troponin I	Aptamer-MoS ₂ nanoconjugates	10 pM to 1.0 μM	0.95 pM	[71]
Electrochemical	Ochratoxin A	NiCo ₂ S ₄ nanoparticle-dispersed MoS ₂ nanosheets	0 to 1 ng mL ⁻¹	0.42 pg mL ⁻¹	[72]
Electrochemical and SERS	Middle East respiratory syndrome coronavirus (MERS-CoV)	DNA aptamer-graphene-MoS ₂	NA	0.645 pg mL ⁻¹ (EIS); 0.525 pg mL ⁻¹ (SERS)	[73]
Electrochemical	Interferon-gamma	Graphene monolayer-based FET	0 nM to 100 μM	83 pM	[75]
Electrochemical	ATP	Graphene monolayer-based FET	0 to 1 mM	10 pM	[76]
Electrochemical	Adenosine monophosphate	Graphene monolayer-based FET	1 nM–100 μM	10 pM	[24]

Table 1. Cont.

Transduction Type	Target	Substances	Dynamic Range	LOD	References
Electrochemical	<i>Salmonella enterica</i>	Graphene oxide–azophloxine nanocomposite	10^1 to 10^8 cfu mL ⁻¹	10^1 cfu mL ⁻¹	[77]
Electrochemical	SARS-CoV-2 nucleocapsid protein	Nanomaterials Au@Pt/MIL-53(Al), DNAzyme, and horseradish peroxidase	0.025 to 50 ng mL ⁻¹	8.33 pg mL ⁻¹	[80]
Electrochemical	ATP	Firefly luciferase activity and gold nanoparticles	1–600 μM	5 μM	[81]
Electrochemical	<i>S. aureus</i>	Teicoplanin (Tcp)-functionalized gold-coated magnet (Fe3O4@Au-Tcp) nanoparticles	7.6×10^1 – 7.6×10^7 CFU mL ⁻¹	1.09 CFU mL ⁻¹	[82]
Electrochemical	MCF-7	TiO ₂ /CdTe heterostructure conjugated to aptamer AS1411	1×10^3 to 1×10^5 cells mL ⁻¹	400 cells mL ⁻¹	[83]
Photoelectrochemical sensor	Thrombin	C60@C3N4 nanocomposites and Au nanoparticles (depAu) decorated perylene tetracarboxylic acid	10 fM to 10 nM	1.5 fM	[85]
Electrochemiluminescence	Carcinoembryonic	CdS quantum dots	100 fg mL ⁻¹ to 10 ng mL ⁻¹	85 fg/mL	[88]
Electrochemiluminescence	Kanamycin detection	g-C3N4-COOH/ZnSe nanocomposite	1.0 nM–100 μM	0.7982 nM	[89]
Electrochemiluminescence	Ochratoxin A	CdTe QDs and cyanine dye (Cy5) fluorophore	0.0005–50 ng mL ⁻¹	0.17 pg mL ⁻¹	[90]
Electrochemiluminescence	Thrombin and Hg ²⁺ detection	Lanthanide ion-doped cadmium sulfide quantum dots	NA	3.00×10^{-13} mol L ⁻¹ for Hg ²⁺ ; 3.00×10^{-17} mol L ⁻¹ for thrombin	[91]

Author Contributions: Conceptualization, S.F., S.G. and M.A.S.; methodology, S.F., S.G. and M.A.S.; investigation, S.F., S.G. and M.A.S.; resources, S.F., S.G. and M.A.S.; data curation; writing—S.F. and S.G.; writing—S.F., S.G., M.A.S. and M.D.; visualization, S.F., S.G., M.D. and M.A.S.; supervision, M.A.S. and M.D.; project administration, M.A.S. and M.D.; funding acquisition, M.A.S. All authors have read and agreed to the published version of the manuscript.

Funding: This research was partially funded by the U.S. National Science Foundation grant number 1303785 and the U.S. Army Research Office (ARO) through MURI Grant No. W911NF-11-1-0024 is acknowledged gratefully.

Conflicts of Interest: The authors declare no conflict of interest.

References

1. Newman, S.; Nakitandwe, J.; Kesserwan, C.A.; Azzato, E.M.; Wheeler, D.A.; Rusch, M.; Shurtleff, S.; Hedges, D.J.; Hamilton, K.V.; Foy, S.G.; et al. Genomes for kids: The scope of pathogenic mutations in pediatric cancer revealed by comprehensive DNA and RNA sequencing. *Cancer Discov.* **2021**, *11*, 3008–3027. [[CrossRef](#)]
2. Peedicayil, J. The role of DNA methylation in the pathogenesis and treatment of cancer. *Curr. Clin. Pharmacol.* **2012**, *7*, 333–340. [[CrossRef](#)]
3. Xing, G.; Zhang, W.; Li, N.; Pu, Q.; Lin, J.-M. Recent progress on microfluidic biosensors for rapid detection of pathogenic bacteria. *Chin. Chem. Lett.* **2022**, *33*, 1743–1751. [[CrossRef](#)]

4. Ko, R.H.H.; Shayegannia, M.; Farid, S.; Kherani, N.P. Protein capture and SERS detection on multiwavelength rainbow-trapping width-graded nano-gratings. *Nanotechnology* **2021**, *32*, 505207.
5. Dinu, A.; Apetrei, C. A review of sensors and biosensors modified with conducting polymers and molecularly imprinted polymers used in electrochemical detection of amino acids: Phenylalanine, tyrosine, and tryptophan. *Int. J. Mol. Sci.* **2022**, *23*, 1218. [[CrossRef](#)]
6. Ellington, A.D.; Szostak, J.W. In vitro selection of RNA molecules that bind specific ligands. *Nature* **1990**, *346*, 818–822. [[CrossRef](#)]
7. Tuerk, C.; Gold, L. Systematic evolution of ligands by exponential enrichment: RNA ligands to bacteriophage T4 DNA polymerase. *Science* **1990**, *249*, 505–510. [[CrossRef](#)]
8. Lan, Y.; Farid, S.; Meshik, X.; Xu, K.; Choi, M.; Ranginwala, S.; Wang, Y.Y.; Burke, P.; Dutta, M.; Stroscio, M.A. Detection of immunoglobulin E with a graphene-based field-effect transistor aptasensor. *J. Sens.* **2018**, *2018*, 3019259. [[CrossRef](#)]
9. Zheng, G.; Zhao, L.; Yuan, D.; Li, J.; Yang, G.; Song, D.; Miao, H.; Shu, J.; Mo, X.; Xu, X.; et al. A genetically encoded fluorescent biosensor for monitoring ATP in living cells with heterobifunctional aptamers. *Biosens. Bioelectron.* **2022**, *198*, 113827. [[CrossRef](#)]
10. Kleinjung, F.; Klussmann, S.; Erdmann, V.A.; Scheller, F.W.; Fürste, J.P.; Bier, F.F. High-affinity RNA as a recognition element in a biosensor. *Anal. Chem.* **1998**, *70*, 328–331. [[CrossRef](#)]
11. Hong, P.; Li, W.; Li, J. Applications of aptasensors in clinical diagnostics. *Sensors* **2012**, *12*, 1181–1193. [[CrossRef](#)]
12. Saberian-Borujeni, M.; Johari-Ahar, M.; Hamzeiy, H.; Barar, J.; Omidi, Y. Nanoscaled aptasensors for multi-analyte sensing. *BioImpacts BI* **2014**, *4*, 205. [[CrossRef](#)]
13. Meshik, X.; Farid, S.; Choi, M.; Lan, Y.; Mukherjee, S.; Datta, D.; Dutta, M.; Stroscio, M.A. Biomedical applications of quantum dots, nucleic acid–based aptamers, and nanostructures in biosensors. *Crit. Rev. Biomed. Eng.* **2015**, *43*, 277–296. [[CrossRef](#)]
14. Charbgoo, F.; Soltani, F.; Taghdisi, S.M.; Abnous, K.; Ramezani, M. Nanoparticles application in high sensitive aptasensor design. *TrAC Trends Anal. Chem.* **2016**, *85*, 85–97. [[CrossRef](#)]
15. Akki, S.U.; Werth, C.J. Critical review: DNA aptasensors, are they ready for monitoring organic pollutants in natural and treated water sources? *Environ. Sci. Technol.* **2018**, *52*, 8989–9007. [[CrossRef](#)]
16. Mishra, G.K.; Sharma, V.; Mishra, R.K. Electrochemical aptasensors for food and environmental safeguarding: A review. *Biosensors* **2018**, *8*, 28. [[CrossRef](#)]
17. Ghorbani, F.; Abbaszadeh, H.; Dolatabadi, J.E.N.; Aghebati-Maleki, L.; Yousefi, M. Application of various optical and electrochemical aptasensors for detection of human prostate specific antigen: A review. *Biosens. Bioelectron.* **2019**, *142*, 111484. [[CrossRef](#)]
18. Yan, S.-R.; Foroughi, M.M.; Safaei, M.; Jahani, S.; Ebrahimpour, N.; Borhani, F.; Baravati, N.R.Z.; Aramesh-Boroujeni, Z.; Foong, L.K. A review: Recent advances in ultrasensitive and highly specific recognition aptasensors with various detection strategies. *Int. J. Biol. Macromol.* **2020**, *155*, 184–207. [[CrossRef](#)]
19. Kim, J.; Noh, S.; Park, J.A.; Park, S.-C.; Park, S.J.; Lee, J.-H.; Ahn, J.-H.; Lee, T. Recent advances in aptasensor for cytokine detection: A review. *Sensors* **2021**, *21*, 8491. [[CrossRef](#)]
20. Margiana, R.; Hammid, A.T.; Ahmad, I.; Alsaikhan, F.; Jalil, A.T.; Tursunbaev, F.; Umar, F.; Parra, R.M.R.; Mustafa, Y.F. Current progress in aptasensor for ultra-low level monitoring of Parkinson’s disease biomarkers. *Crit. Rev. Anal. Chem.* **2022**, *1*–16. [[CrossRef](#)]
21. Komarova, N.; Kuznetsov, A. Inside the black box: What makes SELEX better? *Molecules* **2019**, *24*, 3598. [[CrossRef](#)]
22. Song, S.; Wang, L.; Li, J.; Fan, C.; Zhao, J. Aptamer-based biosensors. *TrAC Trends Anal. Chem.* **2008**, *27*, 108–117. [[CrossRef](#)]
23. Kraly, J.; Fazal, M.A.; Schoenherr, R.M.; Bonn, R.; Harwood, M.M.; Turner, E.; Jones, M.; Dovichi, N.J. Bioanalytical applications of capillary electrophoresis. *Anal. Chem.* **2006**, *78*, 4097–4110. [[CrossRef](#)]
24. Datta, D.; Meshik, X.; Mukherjee, S.; Sarkar, K.; Choi, M.S.; Mazouchi, M.; Farid, S.; Wang, Y.Y.; Burke, P.J.; Dutta, M.; et al. Submillimolar detection of adenosine monophosphate using graphene-based electrochemical aptasensor. *IEEE Trans. Nanotechnol.* **2017**, *16*, 196–202. [[CrossRef](#)]
25. Menger, M.; Yarman, A.; Erdőssy, J.; Yıldız, H.B.; Gyurcsányi, R.E.; Scheller, F.W. MIPs and aptamers for recognition of proteins in biomimetic sensing. *Biosensors* **2016**, *6*, 35. [[CrossRef](#)]
26. Katilius, E.; Carmel, A.B.; Koss, H.; O’Connell, D.; Smith, B.C.; Sanders, G.M.; LaBerge, G.S. Sperm cell purification from mock forensic swabs using SOMAmer™ affinity reagents. *Forensic Sci. Int. Genet.* **2018**, *35*, 9–13. [[CrossRef](#)]
27. Kong, R.-M.; Zhang, X.; Ding, L.; Yang, D.; Qu, F. Label-free fluorescence turn-on aptasensor for prostate-specific antigen sensing based on aggregation-induced emission–silica nanospheres. *Anal. Bioanal. Chem.* **2017**, *409*, 5757–5765. [[CrossRef](#)]
28. Zhang, M.; Guo, X. Emerging strategies in fluorescent aptasensor toward food hazard aflatoxins detection. *Trends Food Sci. Technol.* **2022**, *129*, 621–633. [[CrossRef](#)]
29. Yu, Q.; Dai, Z.; Wu, W.; Zhu, H.; Ji, L. Effects of Different Buffers on the Construction of Aptamer Sensors. In Proceedings of the IOP Conference Series: Materials Science and Engineering, Busan, Republic of Korea, 25–27 August 2017; IOP Publishing: Bristol, UK, 2017; Volume 274, p. 012117.
30. Markvart, T. Light harvesting for quantum solar energy conversion. *Prog. Quantum Electron.* **2000**, *24*, 107–186. [[CrossRef](#)]
31. Sapkota, K.; Dhakal, S. FRET-based aptasensor for the selective and sensitive detection of lysozyme. *Sensors* **2020**, *20*, 914. [[CrossRef](#)]
32. Liu, X.; Wang, T.; Wu, Y.; Tan, Y.; Jiang, T.; Li, K.; Lou, B.; Chen, L.; Liu, Y.; Liu, Z. Aptamer based probes for living cell intracellular molecules detection. *Biosens. Bioelectron.* **2022**, *208*, 114231.

33. Ma, K.; Zhang, F.; Sayyadi, N.; Chen, W.; Anwer, A.G.; Care, A.; Xu, B.; Tian, W.; Goldys, E.M.; Liu, G. “Turn-on” fluorescent aptasensor based on AIEgen labeling for the localization of IFN- γ in live cells. *ACS Sens.* **2018**, *3*, 320–326. [CrossRef]
34. Ma, K.; Xie, W.; Liu, W.; Wang, L.; Wang, D.; Tang, B.Z. Graphene oxide based fluorescent dna aptasensor for liver cancer diagnosis and therapy. *Adv. Funct. Mater.* **2021**, *31*, 2102645. [CrossRef]
35. Xu, J.; Yao, L.; Zhong, X.; Hu, K.; Zhao, S.; Huang, Y. A biodegradable and cofactor self-sufficient aptazyme nanoprobe for amplified imaging of low-abundance protein in living cells. *Talanta* **2023**, *253*, 123983. [CrossRef]
36. Guo, X.-L.; Yuan, D.-D.; Song, T.; Li, X.-M. DNA nanopore functionalized with aptamer and cell-penetrating peptide for tumor cell recognition. *Anal. Bioanal. Chem.* **2017**, *409*, 3789–3797. [CrossRef]
37. Ghosh, S.; Chen, Y.; Sebastian, J.; George, A.; Dutta, M.; Stroscio, M.A. A study on the response of FRET based DNA aptasensors in intracellular environment. *Sci. Rep.* **2020**, *10*, 13250. [CrossRef]
38. Ghosh, S.; Chen, Y.; George, A.; Dutta, M.; Stroscio, M.A. Fluorescence resonant energy transfer-based quantum dot sensor for the detection of calcium ions. *Front. Chem.* **2020**, *8*, 594. [CrossRef]
39. Chen, Z.; Li, H.; Jia, W.; Liu, X.; Li, Z.; Wen, F.; Zheng, N.; Jiang, J.; Xu, D. Bivalent aptasensor based on silver-enhanced fluorescence polarization for rapid detection of lactoferrin in milk. *Anal. Chem.* **2017**, *89*, 5900–5908. [CrossRef]
40. Hendrickson, O.D.; Taranova, N.A.; Zherdev, A.V.; Dzantiev, B.B.; Eremin, S.A. Fluorescence polarization-based bioassays: New horizons. *Sensors* **2020**, *20*, 7132. [CrossRef]
41. Liu, L.; Zhao, Q. A simple fluorescence anisotropy assay for detection of bisphenol A using fluorescently labeled aptamer. *J. Environ. Sci.* **2020**, *97*, 19–24. [CrossRef]
42. Ma, P.; Duan, N.; Ye, H.; Xia, Y.; Ding, Z.; Wang, Z. Selection, truncation and fluorescence polarization based aptasensor for Weissella viridescens detection. *Talanta* **2022**, *246*, 123499. [CrossRef]
43. Ye, H.; Lu, Q.; Duan, N.; Wang, Z. GO-amplified fluorescence polarization assay for high-sensitivity detection of aflatoxin B1 with low dosage aptamer probe. *Anal. Bioanal. Chem.* **2019**, *411*, 1107–1115. [CrossRef]
44. Samokhvalov, A.; Safenkova, I.; Eremin, S.; Zherdev, A.; Dzantiev, B. Use of anchor protein modules in fluorescence polarisation aptamer assay for ochratoxin A determination. *Anal. Chim. Acta* **2017**, *962*, 80–87. [CrossRef]
45. Kang, L.; Yang, B.; Zhang, X.; Cui, L.; Meng, H.; Mei, L.; Wu, C.; Ren, S.; Tan, W. Enzymatic cleavage and mass amplification strategy for small molecule detection using aptamer-based fluorescence polarization biosensor. *Anal. Chim. Acta* **2015**, *879*, 91–96. [CrossRef]
46. Li, Y.; Sun, Y.; Ye, J.; Pan, F.; Peng, B.; Li, H.; Zhang, M.; Xu, Y. Sensitive and selective detection of microRNA in complex biological samples based on protein-enhanced fluorescence anisotropy. *Anal. Methods* **2020**, *12*, 687–692. [CrossRef]
47. Socorro-Leránoz, A.B.; Santano, D.; Del Villar, I.; Matias, I.R. Trends in the design of wavelength-based optical fibre biosensors (2008–2018). *Biosens. Bioelectron. X* **2019**, *1*, 100015. [CrossRef]
48. Park, M.K.; Kee, J.S.; Quah, J.Y.; Netto, V.; Song, J.; Fang, Q.; La Fosse, E.M.; Lo, G.-Q. Label-free aptamer sensor based on silicon microring resonators. *Sens. Actuators B Chem.* **2013**, *176*, 552–559. [CrossRef]
49. Mitin, V.V.; Kochelap, V.A.; Dutta, M.; Stroscio, M.A. *Introduction to Optical and Optoelectronic Properties of Nanostructures*; Cambridge University Press: Cambridge, UK, 2019.
50. Yang, C.J.; Jockusch, S.; Vicens, M.; Turro, N.J.; Tan, W. Light-switching excimer probes for rapid protein monitoring in complex biological fluids. *Proc. Natl. Acad. Sci. USA* **2005**, *102*, 17278–17283. [CrossRef]
51. Dinter, F.; Burdukiewicz, M.; Schierack, P.; Lehmann, W.; Nestler, J.; Dame, G.; Rödiger, S. Simultaneous detection and quantification of DNA and protein biomarkers in spectrum of cardiovascular diseases in a microfluidic microbead chip. *Anal. Bioanal. Chem.* **2019**, *411*, 7725–7735. [CrossRef]
52. Liu, X.; Yang, X.; Li, K.; Liu, H.; Xiao, R.; Wang, W.; Wang, C.; Wang, S. Fe₃O₄@Au SERS tags-based lateral flow assay for simultaneous detection of serum amyloid A and C-reactive protein in unprocessed blood sample. *Sens. Actuators B Chem.* **2020**, *320*, 128350. [CrossRef]
53. Farid, S.; Dixon, K.; Shayegannia, M.; Ko, R.H.H.; Safari, M.; Loh, J.Y.Y.; Kherani, N.P. Rainbows at the end of subwavelength discontinuities: Plasmonic light trapping for sensing applications. *Adv. Opt. Mater.* **2021**, *9*, 2100695. [CrossRef]
54. McCauley, T.G.; Hamaguchi, N.; Stanton, M. Aptamer-based biosensor arrays for detection and quantification of biological macromolecules. *Anal. Biochem.* **2003**, *319*, 244–250. [CrossRef]
55. Cho, E.J.; Collett, J.R.; Szafranska, A.E.; Ellington, A.D. Optimization of aptamer microarray technology for multiple protein targets. *Anal. Chim. Acta* **2006**, *564*, 82–90. [CrossRef]
56. Kirby, R.; Cho, E.J.; Gehrke, B.; Bayer, T.; Park, Y.S.; Neikirk, D.P.; McDevitt, J.T.; Ellington, A.D. Aptamer-based sensor arrays for the detection and quantitation of proteins. *Anal. Chem.* **2004**, *76*, 4066–4075. [CrossRef]
57. Marín, M.J.; Schofield, C.L.; Field, R.A.; Russell, D.A. Glyconanoparticles for colorimetric bioassays. *Analyst* **2015**, *140*, 59–70. [CrossRef]
58. Shayesteh, O.H.; Ghavami, R. A novel label-free colorimetric aptasensor for sensitive determination of PSA biomarker using gold nanoparticles and a cationic polymer in human serum. *Spectrochim. Acta Part A Mol. Biomol. Spectrosc.* **2020**, *226*, 117644. [CrossRef]
59. Shaban, S.M.; Kim, D.-H. Recent advances in aptamer sensors. *Sensors* **2021**, *21*, 979. [CrossRef]
60. Taghdisi, S.M.; Danesh, N.M.; Lavaee, P.; Ramezani, M.; Abnous, K. An aptasensor for selective, sensitive and fast detection of lead (II) based on polyethyleneimine and gold nanoparticles. *Environ. Toxicol. Pharmacol.* **2015**, *39*, 1206–1211. [CrossRef]

61. Priyadarshni, N.; Nath, P.; Nagahnumaiah; Chanda, N. DMSA-functionalized gold nanorod on paper for colorimetric detection and estimation of arsenic (III and V) contamination in groundwater. *ACS Sustain. Chem. Eng.* **2018**, *6*, 6264–6272. [[CrossRef](#)]
62. Li, H.; Rothberg, L. Colorimetric detection of DNA sequences based on electrostatic interactions with unmodified gold nanoparticles. *Proc. Natl. Acad. Sci. USA* **2004**, *101*, 14036–14039. [[CrossRef](#)]
63. Guo, L.; Jackman, J.A.; Yang, H.-H.; Chen, P.; Cho, N.-J.; Kim, D.-H. Strategies for enhancing the sensitivity of plasmonic nanosensors. *Nano Today* **2015**, *10*, 213–239. [[CrossRef](#)]
64. Wei, Y.; Wang, D.; Zhang, Y.; Sui, J.; Xu, Z. Multicolor and photothermal dual-readout biosensor for visual detection of prostate specific antigen. *Biosens. Bioelectron.* **2019**, *140*, 111345. [[CrossRef](#)]
65. Sassolas, A.; Blum, L.J.; Leca-Bouvier, B.D. Electrochemical aptasensors. *Electroanal. Int. J. Devoted Fundam. Pract. Asp. Electroanal.* **2009**, *21*, 1237–1250. [[CrossRef](#)]
66. Lei, Z.; Lei, P.; Guo, J.; Wang, Z. Recent advances in nanomaterials-based optical and electrochemical aptasensors for detection of cyanotoxins. *Talanta* **2022**, *248*, 123607. [[CrossRef](#)]
67. Ikebukuro, K.; Kiyohara, C.; Sode, K. Electrochemical detection of protein using a double aptamer sandwich. *Anal. Lett.* **2004**, *37*, 2901–2909. [[CrossRef](#)]
68. Majdinasab, M.; Marty, J.L. Recent advances in electrochemical aptasensors for detection of biomarkers. *Pharmaceuticals* **2022**, *15*, 995. [[CrossRef](#)]
69. Bao, Y.; Ye, S.; Zhou, C.; Chen, L. Molybdenum (IV) sulfide nanosheet-based aptasensor for the label-free determination of bisphenol A (BPA) by electrochemical impedance spectroscopy (EIS). *Anal. Lett.* **2022**, *55*, 1971–1979. [[CrossRef](#)]
70. Karim, S.S.; Sudais, A.; Shah, M.S.; Farrukh, S.; Ali, S.; Ahmed, M.; Salahuddin, Z.; Fan, X. A contemplating review on different synthesis methods of 2D-Molybdenum disulfide (MoS₂) nanosheets. *Fuel* **2023**, *351*, 128923. [[CrossRef](#)]
71. Qiao, X.; Li, K.; Xu, J.; Cheng, N.; Sheng, Q.; Cao, W.; Yue, T.; Zheng, J. Novel electrochemical sensing platform for ultrasensitive detection of cardiac troponin I based on aptamer-MoS₂ nanoconjugates. *Biosens. Bioelectron.* **2018**, *113*, 142–147. [[CrossRef](#)]
72. Gao, H.; Yao, J.; Jiang, B.; Yuan, R.; Xiang, Y. NiCo₂S₄ nanoparticle-dispersed MoS₂ nanosheets for catalytic and sensitive electrochemical aptamer sensing of ochratoxin A via cascaded amplifications. *Sens. Actuators B Chem.* **2022**, *371*, 132530. [[CrossRef](#)]
73. Kim, G.; Kim, J.; Kim, S.M.; Kato, T.; Yoon, J.; Noh, S.; Park, E.Y.; Park, C.; Lee, T.; Choi, J.-W. Fabrication of MERS-nanovesicle biosensor composed of multi-functional DNA aptamer/graphene-MoS₂ nanocomposite based on electrochemical and surface-enhanced Raman spectroscopy. *Sens. Actuators B Chem.* **2022**, *352*, 131060. [[CrossRef](#)]
74. Centane, S.; Nyokong, T. Co phthalocyanine mediated electrochemical detection of the HER2 in the presence of Au and CeO₂ nanoparticles and graphene quantum dots. *Bioelectrochemistry* **2023**, *149*, 108301. [[CrossRef](#)]
75. Farid, S.; Meshik, X.; Choi, M.; Mukherjee, S.; Lan, Y.; Parikh, D.; Poduri, S.; Baterdene, U.; Huang, C.-E.; Wang, Y.Y.; et al. Detection of Interferon gamma using graphene and aptamer based FET-like electrochemical biosensor. *Biosens. Bioelectron.* **2015**, *71*, 294–299. [[CrossRef](#)]
76. Mukherjee, S.; Meshik, X.; Choi, M.; Farid, S.; Datta, D.; Lan, Y.; Poduri, S.; Sarkar, K.; Baterdene, U.; Huang, C.-E.; et al. A graphene and aptamer based liquid gated FET-like electrochemical biosensor to detect adenosine triphosphate. *IEEE Trans. Nanobioscience* **2015**, *14*, 967–972. [[CrossRef](#)]
77. Appaturi, J.N.; Pulingam, T.; Thong, K.L.; Muniandy, S.; Ahmad, N.; Leo, B.F. Rapid and sensitive detection of Salmonella with reduced graphene oxide-carbon nanotube based electrochemical aptasensor. *Anal. Biochem.* **2020**, *589*, 113489. [[CrossRef](#)]
78. Muniandy, S.; Dinshaw, I.J.; Teh, S.J.; Lai, C.W.; Ibrahim, F.; Thong, K.L.; Leo, B.F. Graphene-based label-free electrochemical aptasensor for rapid and sensitive detection of foodborne pathogen. *Anal. Bioanal. Chem.* **2017**, *409*, 6893–6905. [[CrossRef](#)]
79. Richa, S.; Ragavan, K.V.; Thakur, M.S.; Raghavarao, K.S.M.S. Recent advances in nanoparticle based aptasensors for food contaminants. *Biosens. Bioelectron.* **2015**, *74*, 612–627.
80. Tian, J.; Liang, Z.; Hu, O.; He, Q.; Sun, D.; Chen, Z. An electrochemical dual-aptamer biosensor based on metal-organic frameworks MIL-53 decorated with Au@Pt nanoparticles and enzymes for detection of COVID-19 nucleocapsid protein. *Electrochim. Acta* **2021**, *387*, 138553. [[CrossRef](#)]
81. Karimi, E.; Nikkhah, M.; Hosseinkhani, S. Label-Free and Bioluminescence-Based Nano-Biosensor for ATP Detection. *Biosensors* **2022**, *12*, 918. [[CrossRef](#)]
82. Qi, X.; Ye, Y.; Wang, H.; Zhao, B.; Xu, L.; Zhang, Y.; Wang, X.; Zhou, N. An ultrasensitive and dual-recognition SERS biosensor based on Fe₃O₄@Au-Teicoplanin and aptamer functionalized Au@Ag nanoparticles for detection of *Staphylococcus aureus*. *Talanta* **2022**, *250*, 123648. [[CrossRef](#)]
83. Wang, K.; Zhang, R.; Sun, N.; Li, X.; Wang, J.; Cao, Y.; Pei, R. Near-infrared light-driven photoelectrochemical aptasensor based on the upconversion nanoparticles and TiO₂/CdTe heterostructure for detection of cancer cells. *ACS Appl. Mater. Interfaces* **2016**, *8*, 25834–25839. [[CrossRef](#)]
84. Liu, G.; Mao, X.; Phillips, J.A.; Xu, H.; Tan, W.; Zeng, L. Aptamer-nanoparticle strip biosensor for sensitive detection of cancer cells. *Anal. Chem.* **2009**, *81*, 10013–10018. [[CrossRef](#)]
85. Yang, L.; Zhong, X.; Huang, L.; Deng, H.; Yuan, R.; Yuan, Y. C₆₀@C₃N₄ nanocomposites as quencher for signal-off photoelectrochemical aptasensor with Au nanoparticle decorated perylene tetracarboxylic acid as platform. *Anal. Chim. Acta* **2019**, *1077*, 281–287. [[CrossRef](#)]
86. Miao, W. Electrogenerated chemiluminescence and its biorelated applications. *Chem. Rev.* **2008**, *108*, 2506–2553. [[CrossRef](#)]

87. Kurup, C.P.; Lim, S.A.; Ahmed, M.U. Nanomaterials as signal amplification elements in aptamer-based electrochemiluminescent biosensors. *Bioelectrochemistry* **2022**, *147*, 108170.
88. Wei, X.-h.; Qiao, X.; Fan, J.; Hao, Y.-Q.; Zhang, Y.-T.; Zhou, Y.-L.; Xu, M.-T. A label-free ECL aptasensor for sensitive detection of carcinoembryonic antigen based on CdS QDs@MOF and TEOA@Au as bi-coreactants of Ru (bpy) 32+. *Microchem. J.* **2022**, *173*, 106910. [[CrossRef](#)]
89. Liu, X.-P.; Cheng, J.-L.; Mao, C.-J.; Wu, M.-Z.; Chen, J.-S.; Jin, B.-K. Highly sensitive electrochemiluminescence aptasensor based on a g-C₃N₄-COOH/ZnSe nanocomposite for kanamycin detection. *Microchem. J.* **2022**, *172*, 106928. [[CrossRef](#)]
90. Gao, J.; Chen, Z.; Mao, L.; Zhang, W.; Wen, W.; Zhang, X.; Wang, S. Electrochemiluminescent aptasensor based on resonance energy transfer system between CdTe quantum dots and cyanine dyes for the sensitive detection of Ochratoxin A. *Talanta* **2019**, *199*, 178–183. [[CrossRef](#)]
91. Wang, C.; Chen, M.; Wu, J.; Mo, F.; Fu, Y. Multi-functional electrochemiluminescence aptasensor based on resonance energy transfer between Au nanoparticles and lanthanum ion-doped cadmium sulfide quantum dots. *Anal. Chim. Acta* **2019**, *1086*, 66–74. [[CrossRef](#)]
92. Grabowska, I.; Hepel, M.; Kurzatkowska-Adaszynska, K. Advances in design strategies of multiplex electrochemical aptasensors. *Sensors* **2021**, *22*, 161. [[CrossRef](#)]
93. Popov, A.; Brasius, B.; Kausaite-Minkstiene, A.; Ramanaviciene, A. Metal nanoparticle and quantum dot tags for signal amplification in electrochemical immunosensors for biomarker detection. *Chemosensors* **2021**, *9*, 85. [[CrossRef](#)]
94. Xiang, J.; Pi, X.; Chen, X.; Xiang, L.; Yang, M.; Ren, H.; Shen, X.; Qi, N.; Deng, C. Integrated signal probe based aptasensor for dual-analyte detection. *Biosens. Bioelectron.* **2017**, *96*, 268–274. [[CrossRef](#)]
95. Pakchin, P.S.; Nakhjavani, S.A.; Saber, R.; Ghanbari, H.; Omidi, Y. Recent advances in simultaneous electrochemical multi-analyte sensing platforms. *TrAC Trends Anal. Chem.* **2017**, *92*, 32–41. [[CrossRef](#)]
96. Shayesteh, O.H.; Khosroshahi, A.G. A polyA aptamer-based label-free colorimetric biosensor for the detection of kanamycin in human serum. *Anal. Methods* **2020**, *12*, 1858–1867. [[CrossRef](#)]
97. Raouafi, A.; Sánchez, A.; Raouafi, N.; Villalonga, R. Electrochemical aptamer-based bioplatform for ultrasensitive detection of prostate specific antigen. *Sens. Actuators B Chem.* **2019**, *297*, 126762. [[CrossRef](#)]
98. Li, P.; Yu, X.; Han, W.; Kong, Y.; Bao, W.; Zhang, J.; Zhang, W.; Gu, Y. Ultrasensitive and reversible nanoplatform of urinary exosomes for prostate cancer diagnosis. *ACS Sens.* **2019**, *4*, 1433–1441. [[CrossRef](#)]
99. Heathman, T.R.J.; Rafiq, Q.A.; Chan, A.K.C.; Coopman, K.; Nienow, A.W.; Kara, B.; Hewitt, C.J. Characterization of human mesenchymal stem cells from multiple donors and the implications for large scale bioprocess development. *Biochem. Eng. J.* **2016**, *108*, 14–23. [[CrossRef](#)]

Disclaimer/Publisher's Note: The statements, opinions and data contained in all publications are solely those of the individual author(s) and contributor(s) and not of MDPI and/or the editor(s). MDPI and/or the editor(s) disclaim responsibility for any injury to people or property resulting from any ideas, methods, instructions or products referred to in the content.